



# Identifying complex Fermi resonances in *p*-difluorobenzene using zero-electron-kinetic-energy (ZEKE) spectroscopy

Cite as: J. Chem. Phys. **149**, 094301 (2018); <https://doi.org/10.1063/1.5045544>

Submitted: 21 June 2018 . Accepted: 17 August 2018 . Published Online: 05 September 2018

David J. Kemp, Adrian M. Gardner, William D. Tuttle, Jonathan Midgley, Katharine L. Reid , and Timothy G. Wright 



View Online



Export Citation



CrossMark

## ARTICLES YOU MAY BE INTERESTED IN

[Perspective: The development and applications of H Rydberg atom translational spectroscopy methods](#)

The Journal of Chemical Physics **149**, 080901 (2018); <https://doi.org/10.1063/1.5047911>

[Coulomb explosion imaging of CH<sub>3</sub>I and CH<sub>2</sub>ClI photodissociation dynamics](#)

The Journal of Chemical Physics **149**, 204313 (2018); <https://doi.org/10.1063/1.5041381>

[Complexity surrounding an apparently simple Fermi resonance in \*p\*-fluorotoluene revealed using two-dimensional laser-induced fluorescence \(2D-LIF\) spectroscopy](#)

The Journal of Chemical Physics **150**, 064306 (2019); <https://doi.org/10.1063/1.5083682>



Lock-in Amplifiers

Zurich Instruments

Watch the Video

# Identifying complex Fermi resonances in *p*-difluorobenzene using zero-electron-kinetic-energy (ZEKE) spectroscopy

David J. Kemp, Adrian M. Gardner,<sup>a)</sup> William D. Tuttle, Jonathan Midgley, Katharine L. Reid, and Timothy G. Wright<sup>b)</sup>  
*School of Chemistry, University of Nottingham, University Park, Nottingham NG7 2RD, United Kingdom*

(Received 21 June 2018; accepted 17 August 2018; published online 5 September 2018)

The vibrations of the ground state cation ( $\tilde{X}^2B_{2g}$ ) of *para*-difluorobenzene (*p*DFB) have been investigated using zero-electron-kinetic-energy (ZEKE) spectroscopy. A comprehensive set of ZEKE spectra were recorded via different vibrational levels of the  $S_1$  state ( $<0^0 + 1300\text{ cm}^{-1}$ ). The adiabatic ionization energy for *p*DFB was measured as  $73\,869 \pm 5\text{ cm}^{-1}$ . Use of different intermediate levels allows different cationic vibrational activity to be obtained via the modification of the Franck-Condon factors for the ionization step, allowing the wavenumbers of different vibrational levels in the cation to be established. In addition, assignment of the vibrational structure in the ZEKE spectra allowed interrogation of the assignments of the  $S_1 \leftarrow S_0$  transition put forward by Knight and Kable [J. Chem. Phys. **89**, 7139 (1988)]. Assignment of the vibrational structure has been aided by quantum chemical calculations. In this way, it was possible to assign seventeen of the thirty vibrational modes of the ground state *p*DFB<sup>+</sup> cation. Evidence for complex Fermi resonances in the  $S_1$  state, i.e., those that involve more than two vibrations, was established. One of these was investigated using picosecond time-resolved photoelectron spectroscopy. In addition, we discuss the appearance of several symmetry-forbidden bands in the ZEKE spectra, attributing their appearance to a Rydberg state variation of an intrachannel vibronic coupling mechanism. *Published by AIP Publishing.* <https://doi.org/10.1063/1.5045544>

## I. INTRODUCTION

The *p*-difluorobenzene (*p*DFB) molecule is a prototypical  $D_{2h}$  point-group symmetry molecule and is a useful probe of the effect of a symmetric *para* disubstitution on the  $\pi$ -orbital system of the  $D_{6h}$  symmetry benzene molecule. The outermost electronic configuration is  $\dots b_{3u}^2 b_{1g}^2 b_{2g}^2 a_u^0$  for *p*DFB and so it may thus be seen that the lowest energy  $a_u \leftarrow b_{2g}$  excitation gives rise to the  $\tilde{A}^1B_{2u}$  electronic state (denoted  $S_1$ ), and the lowest-energy ionization yields the  $\tilde{X}^2B_{2g}$  ground state cation (denoted  $D_0^+$ ).

The  $S_1 \leftarrow S_0$  transition has been studied in depth by Cooper,<sup>1</sup> Robey and Schlag (RS),<sup>2</sup> Coveleskie and Parmenter (CP),<sup>3</sup> and particularly by Knight and Kable (KK).<sup>4</sup> Cooper's study<sup>1</sup> was via one-photon absorption, with vibrational progressions being identified and assignments to some totally symmetric modes being made. RS<sup>2</sup> employed two-photon absorption spectroscopy of a room-temperature gaseous sample, using both linearly and circularly polarized light. CP<sup>3</sup> and KK<sup>4</sup> each used laser-induced fluorescence (LIF), with the assignments also being interrogated by dispersed fluorescence (DF), with CP employing a room temperature gaseous sample and KK using a jet-cooled sample. As a result of these studies, many of the  $S_1$  vibrational wavenumbers have been established. The KK study<sup>4</sup> has the most comprehensive set of

$S_1$  vibrational wavenumbers, which are summarized in Table I, where several values are in poor agreement with the calculated values. Parmenter and co-workers have also studied *p*DFB with a view to comparing to the behavior of *para*-fluorotoluene (*p*FT) in investigations of the effect on intramolecular vibrational redistribution (IVR) caused by a methyl group—see, for example, Ref. 5.

The photoelectron spectrum of *p*DFB has been reported by a number of workers, with laser-based photoelectron spectroscopy (PES) studies including the REMPI-PES studies of Sekreta *et al.*<sup>6</sup> and Bellm and Reid,<sup>7</sup> and the zero-electron-kinetic-energy (ZEKE) study of Müller-Dethlefs and co-workers.<sup>8,9</sup> In addition, there are two-colour mass-analyzed threshold ionization (MATI) spectra from Lembach and Brutschy,<sup>10</sup> recorded as part of their study of vibrational predissociation in the *p*DFB-Ar complex. Finally, a one-photon MATI study by Kwon *et al.*<sup>11</sup> has been reported, where the ionization occurs directly from the neutral ground state,  $S_0$ . These studies have provided wavenumber values for a number of ground state cation vibrations, which are summarized in Table I. A number of these values are in disagreement, and so there is still uncertainty regarding some of the assignments. We note that: the REMPI-PES studies of Sekreta *et al.*<sup>6</sup> and Bellm and Reid<sup>7</sup> suffer from reduced resolution compared to the other studies; the ZEKE and MATI studies of Reiser *et al.*<sup>9</sup> and Lembach and Brutschy<sup>10</sup> employ only a limited number of intermediate levels; and the MATI study of Kwon *et al.*<sup>11</sup> is limited by the fact that it is a single-photon method, and so resonant intermediate levels cannot be employed in order to vary the Franck-Condon activity—i.e.,

<sup>a)</sup>Present address: Stephenson Institute for Renewable Energy, University of Liverpool, Liverpool L69 7ZF, United Kingdom.

<sup>b)</sup>Author to whom correspondence should be addressed: Tim.Wright@nottingham.ac.uk

TABLE I. Calculated and experimental vibrational wavenumbers ( $\text{cm}^{-1}$ ) for the  $S_0$ ,  $S_1$ , and  $D_0^+$  electronic states of *p*DFB.

$D_i^a$	Mulliken ( $D_{2h}$ ) <sup>b</sup>	Wilson/Varsányi labels <sup>c</sup>	Duschinsky <sup>d</sup>	$S_0$		$S_1$			$D_0^+$				
				Expt. <sup>e</sup>	Calc. <sup>f</sup>	Expt. <sup>g</sup>	Expt. (this work)	Calc. <sup>h</sup>	Expt. <sup>i</sup>	Expt. <sup>j</sup>	Expt. <sup>k</sup>	Expt. (this work)	Calc. <sup>l</sup>
$D_1$	1( $a_g$ )	2	<b>2,7a</b>	3088	3114			3143	3098		3015		3118
$D_2$	10( $b_{1u}$ )	20a	<b>13,20a</b>	3073	3100			3131			3094		3108
$D_3$	2( $a_g$ )	8a	<b>9a</b>	1615	1595			1519	1640	1600	1640	1642	1628
$D_4$	11( $b_{1u}$ )	19a	<b>18a,(20a)</b>	1514	1492	1335		1422					1457
$D_5$	3( $a_g$ )	7a	1,7a,(2,6a)	1257	1226	1251	1256	1235	1375	1340	1379	1377	1350
$D_6$	12( $b_{1u}$ )	13	12,19a,20a,(13 18a)	1228	1187	1015		1198					1274
$D_7$	4( $a_g$ )	9a	<b>8a</b>	1140	1126	[1116] <sup>m</sup>	1114	1099	1148	1110	1152	1152	1137
$D_8$	13( $b_{1u}$ )	18a	<b>19a,12</b>	1014	999	937		951			983		956
$D_9$	5( $a_g$ )	1	1,6a,(7a,2)	859	841	818	818	820	836	830	839	839	823
$D_{10}$	14( $b_{1u}$ )	12	20a,12,(19a,13)	740	724	[666] <sup>m</sup>		710			743/731 <sup>n</sup>		726
$D_{11}$	6( $a_g$ )	6a	<b>6a,7a,(2,1)</b>	450	443	410	411	414	439	430	441	441	435
$D_{12}$	7( $a_u$ )	17a	<b>17a</b>	945	939	583	585	501			1015 <sup>o</sup>	980	972
$D_{13}$	9( $b_{1g}$ )	10a	<b>10a</b>	800	792	475 <sup>p</sup>	477	429	726 <sup>q</sup>		768	765	760
$D_{14}$	8( $a_u$ )	16a	<b>16a</b>	422	424	175	168	97 <sup>r</sup>	359	350	368 <sup>s</sup>	361	360
$D_{15}$	15( $b_{2g}$ )	5	<b>5,10b</b>	928	927	670	660	697			1015 <sup>o</sup>	955	978
$D_{16}$	28( $b_{3u}$ )	11	<b>17b,11,(16b)</b>	838	835	619	626	667	859			845	864
$D_{17}$	16( $b_{2g}$ )	4	<b>4,(10b)</b>	692	694	528	529	567			743/731 <sup>n</sup>	730	710
$D_{18}$	29( $b_{3u}$ )	16b	<b>16b,11,(17b)</b>	505	505	438	440	487	508	510	515	512	506
$D_{19}$	17( $b_{2g}$ )	10b	<b>10b,4,(5)</b>	374	363	274	273	279	303		303	305	289
$D_{20}$	30( $b_{3u}$ )	17b	16b,17b,11	158	154	120	120	124	127	130	124	127	123
$D_{21}$	18( $b_{2u}$ )	20b	<b>20b</b>	3091	3113			3139					3117
$D_{22}$	23( $b_{3g}$ )	7b	<b>7b</b>	3085	3102			3126			3054		3109
$D_{23}$	24( $b_{3g}$ )	8b	<b>9b</b>	1617	1601	1516		1407			1459		1388
$D_{24}$	19( $b_{2u}$ )	19b	<b>18b,(19b,14,15)</b>	1437	1400			1397			1526		1472
$D_{25}$	20( $b_{2u}$ )	14	<b>15,(14)</b>	1306	1287	1591		1317			1351		1311
$D_{26}$	25( $b_{3g}$ )	9b	<b>3,8b</b>	1285	1268	[933] <sup>m</sup>		1232			1278		1238
$D_{27}$	21( $b_{2u}$ )	15	<b>14,19b</b>	1085	1074	1100		1022			1113		1096
$D_{28}$	26( $b_{3g}$ )	6b	<b>6b,(8b)</b>	635	628	558	558	553			583	584	572
$D_{29}$	27( $b_{3g}$ )	3	8b,6b,(3)	446	435	403	401	396	430			429	424
$D_{30}$	22( $b_{2u}$ )	18b	19b,14,18b	348	337	352	355	347			368 <sup>s</sup>	369	357

<sup>a</sup>See Ref. 25 for the form of these vibrations and further discussion.<sup>b</sup>Mulliken<sup>30</sup>/Herzberg<sup>31</sup> numbering.<sup>c</sup>Given as Wilson labels in Ref. 4 without any detailed comment.<sup>d</sup>Normal modes of *p*DFB expressed in terms of those of benzene using a generalized Duschinsky approach, where the bold denotes a dominant contribution—see Ref. 25.<sup>e</sup>Evaluated set of values discussed in Ref. 25.<sup>f</sup>B3LYP/aug-cc-pVTZ scaled by 0.97.<sup>25</sup><sup>g</sup>LIF values from Ref. 4.<sup>h</sup>TD-B3LYP/aug-cc-pVTZ scaled by 0.97.<sup>27</sup><sup>i</sup>Two-colour ZEKE spectroscopy.<sup>9</sup><sup>j</sup>Two-colour REMPI-PES spectroscopy.<sup>6</sup><sup>k</sup>One-colour MATI spectroscopy.<sup>11</sup><sup>l</sup>UB3LYP/aug-cc-pVTZ scaled by 0.97.<sup>27</sup> These results are in excellent agreement with the B3LYP/6-311++G(2df,2pd) values of Ref. 11 (we assumed these were unrestricted also), particularly if those values are scaled by 0.97 also.<sup>m</sup>These assignments were not supported by DF spectra in Ref. 4.<sup>n</sup>In Ref. 11, it was not possible to decide between the assignment of one or the other of these values to  $D_{10}$  or  $D_{17}$ .<sup>o</sup>In Ref. 11, it was not possible to decide between the assignment of this value to  $D_{12}$  or  $D_{15}$ .<sup>p</sup>In Ref. 4, two possible assignments for  $D_{13}$  were put forward:  $588 \text{ cm}^{-1}$  and  $475 \text{ cm}^{-1}$ . As we noted in Ref. 27, the lower value is in better agreement with the calculated value, and herein we have seen that the ZEKE spectra also support this lower value—see text.<sup>q</sup>We believe this assignment to be incorrect—see text.<sup>r</sup>The calculated value for  $D_{14}$  in the  $S_1$  state using TD-B3LYP is highly unreliable—see Refs. 26, 27, and 35.<sup>s</sup>In Ref. 11, it was not possible to decide between the assignment of this value to  $D_{14}$  or  $D_{30}$ .

just a single MATI spectrum is obtained from the  $S_0$  vibrationless level. It is the aim of the present work to carry out a comprehensive study of the  $S_1$  vibrational levels by recording ZEKE spectra via all significant intermediate levels observed in the  $S_1 \leftarrow S_0$  excitation, below  $1300 \text{ cm}^{-1}$ . This will allow a large variation of the Franck-Condon factors for the ionization step to be achieved. Furthermore, comparison of the

observed activity following projection of the population of the  $S_1$  state onto the ground state neutral (DF in Ref. 4) and cation (ZEKE, this work) levels should provide further evidence for the assignments, particularly the occurrence of Fermi resonances.

Information on the ground state cation and its excited states has been obtained by Bondybey *et al.* by electronic

absorption spectroscopy in an inert matrix,<sup>12</sup> and by Ito and co-workers<sup>13,14</sup> via a variant of two-colour REMPI spectroscopy, termed mass-selected ion-dip spectroscopy. Furthermore, complete-active space calculations including second-order perturbative treatment of dynamic electron correlation (CASPT2) on the low-lying electronic states of the *p*DFB cation have been reported by Yu and Huang.<sup>15</sup>

We shall also report time-resolved photoelectron spectra using picosecond laser pulses, with which vibrational resolution can be achieved.<sup>16–18</sup>

## II. EXPERIMENTAL

The REMPI and ZEKE apparatus employed has been described previously in detail elsewhere.<sup>19,20</sup> The *p*DFB vapour above a room temperature sample was seeded in  $\sim 1.5$  bars of Ar and the gaseous mixture passed through a general valve pulsed nozzle ( $750\ \mu\text{m}$ , 10 Hz, opening time of 180–210  $\mu\text{s}$ ) to create a free jet expansion. The excitation and ionization sources were dye lasers (Sirah Cobra-Stretch) operating with C540A or C503, depending on the energetic region of interest. The two dye lasers were pumped by either a Surelite I or Surelite III Nd:YAG laser, which varied in different experiments. The third harmonic (355 nm) was used to pump the dye lasers, and their fundamental frequencies were frequency doubled using  $\beta$ -barium borate (BBO) crystals. These frequency-doubled outputs were focused and overlapped temporally and spatially—coaxially and counterpropagating—in the centre of a vacuum chamber. Here, they intersected the free jet expansion between two biased electrical grids located in the extraction region of a time-of-flight mass spectrometer, which was employed in the REMPI experiments. These grids were also used in the ZEKE experiments by application of pulsed voltages, giving typical fields ( $F$ ) of  $\sim 10\ \text{V cm}^{-1}$ , after a delay of up to 2  $\mu\text{s}$ , where this delay was minimized while avoiding the introduction of excess noise from the prompt electron signal. ZEKE bands had widths of  $\sim 5\text{--}7\ \text{cm}^{-1}$ , even when  $\sqrt{F}$  relationships would suggest the widths should be significantly greater, because of the well-known decay of the lower-lying Rydberg states accessed in the pulsed-field ionization process.<sup>21</sup> Where possible, we excited in the “dip” in the centre of a REMPI band, which should correspond to the lowest rotational energy levels, and so produce narrow ZEKE bands.

The picosecond time-resolved photoelectron imaging apparatus has been described previously,<sup>22</sup> and a study of the higher-wavenumber  $5^1 9^1$  bands in *p*DFB has been reported.<sup>23</sup> In brief, two independently tuneable, vertically polarized UV laser beams were produced from the frequency-doubled outputs of two optical paramagnetic amplifiers (*light conversion*), pumped by a picosecond Ti:sapphire laser system (*coherent*). A UV pulse duration of 1 ps, corresponding to a bandwidth of  $13\ \text{cm}^{-1}$ , was employed for both the pump and probe. One of these UV outputs prepared a wavepacket in the  $S_1$  state by the coherent excitation of a superposition of eigenstates, and then the second, spatially overlapped and counterpropagating, ionized the evolving superposition after a variable time delay ( $-20$  to  $+250$  ps), which was controlled by a motorized delay stage (Standa). Photoelectron images were obtained using a

velocity-map imaging spectrometer,<sup>7</sup> and the time-resolved spectra were obtained from the measured images.<sup>24</sup>

## III. RESULTS AND DISCUSSION

In Table I, we show calculated wavenumbers for *p*DFB in the  $S_0$ ,  $S_1$ , and  $D_0^+$  states; in addition, we have also included the experimental values, where available—a number of which are established or confirmed in the present work. The experimental and calculated wavenumbers for the  $S_0$  state are discussed in depth in Ref. 25. The calculated wavenumbers for the  $S_1$  and  $D_0^+$  states are taken from Refs. 26 and 27, where comparisons were made to available experimental values and those of the vibrations of *p*F<sub>7</sub>T and *para*-xylene (*p*Xyl). In the present work, we shall discuss some of the  $S_0$  and  $S_1$  assignments in the light of the ZEKE spectra including the identification of Fermi resonances, via the activities of vibrations in the  $D_0^+$  state.

### A. REMPI spectrum

In Fig. 1, we show the REMPI spectrum of *p*DFB in the range  $0\text{--}1300\ \text{cm}^{-1}$ . The spectrum has been calibrated to agree with the absorption spectrum presented by Cvitaš and Hollas,<sup>28</sup> with the  $S_1 0^0$  origin wavenumber at  $36\ 837.9\ \text{cm}^{-1}$ . The REMPI spectrum is not normalized to the UV intensity but looks very similar to the corresponding portion of the LIF spectrum presented in Ref. 4, both with regard to band positions and relative intensities. It is notable that the origin and a number of totally symmetric vibrations, such as  $11^1$ ,  $9^1$ , and  $5^1$ , are significant contributors. The assignments given in Fig. 1 are discussed below, where expanded views of some sections of the spectrum are presented.

Since there are a large number of ZEKE spectra to discuss, we split these into groups according to their energetic proximity and activity. In each case, we shall also discuss the assignments in the light of the DF spectra of KK.<sup>4</sup> In previous work, we have also highlighted the correspondence in vibrational activity for REMPI and ZEKE spectra of similar molecules,<sup>29</sup> if a consistent labelling scheme for the vibrations is employed; hence, the  $D_i$  labels of Ref. 25 are employed in the present study, and the forms of the vibrations, and further discussion, can be found in that work. In earlier work, both Mulliken<sup>30</sup>/Herzberg<sup>31</sup> and Wilson<sup>32</sup>/Varsányi<sup>33</sup> labels have been employed. In referring to previous studies, we will also employ the  $D_i$  labels of Ref. 25, and to aid the reader, the correspondence between the different labels is given in Table I.

Note that almost all transitions will commence from the  $S_0$  zero-point level for our jet-cooled sample, and so the lower vibrational level is omitted when denoting transitions. (For succinctness, we shall often refer to a “level” by using the notation of a transition—in such cases, the “level” refers to the upper one of the transition.) An exception is hot bands (marked with red dots in Fig. 1), where we will explicitly indicate the lower level for clarity. Thus, in Fig. 1, we can see that there is a persistent vibrational hot band at  $-100\ \text{cm}^{-1}$ , which may be assigned to the  $19_1^1$  transition in agreement with Cvitaš and Hollas,<sup>28</sup> this band is rotationally cold, as judged by its

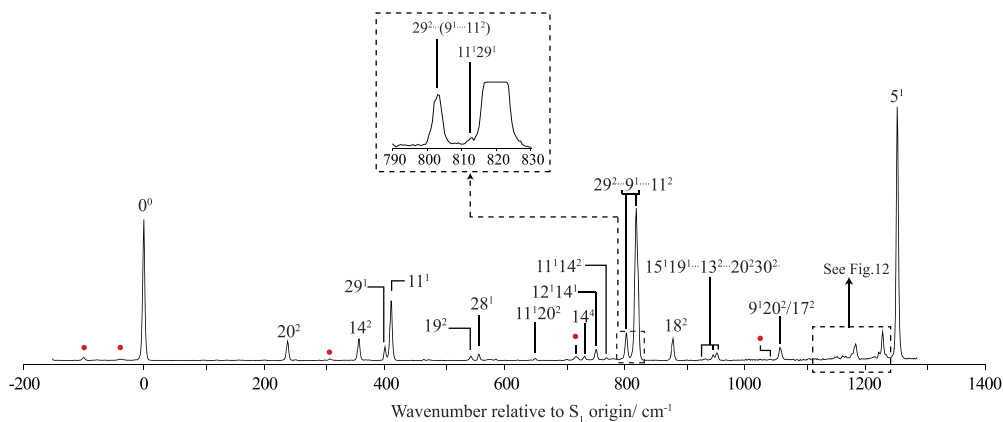


FIG. 1. Two-colour ( $1 + 1'$ ) REMPI spectrum of the 0–1300  $\text{cm}^{-1}$  region of the  $p\text{DFB } S_1 \leftarrow S_0$  transition. Hot band positions are identified with a red dot. The assignments are discussed in the text.

narrowness, but interestingly it is difficult to cool out this vibrational hot band feature associated with the  $D_{19}$  vibration. There are also weaker features at  $-36 \text{ cm}^{-1}$  and  $-41 \text{ cm}^{-1}$ , which may be assigned to  $20_1^1$  and  $11_1^1$ , with the former assignment in agreement with CP;<sup>3</sup> it is also possible that there is a contribution from  $p\text{DFB-Ar}$  to these latter features. We shall see that the more-intense  $19_1^1$  transition is responsible for the presence of other hot bands seen in the REMPI spectrum, which we shall highlight below. No clear evidence has been found of contributions related to the other hot band features.

In the ZEKE spectra, the assignments of the most intense and other pertinent bands are indicated; however, we refrain from labelling every single weak band, many of which appear more intensely in other spectra.

## B. ZEKE spectra via $S_1 0^0$ and “accidental” resonances

In Fig. 2(a), we show a ZEKE spectrum recorded via the  $S_1$  origin transition,  $0^0$ . The corresponding ZEKE spectra were presented in Refs. 8 and 9 and are similar in appearance, but we present a more expanded version here; in addition, our ZEKE spectrum looks similar to the limited range reported in the corresponding MATI spectrum of Lembach and Brutschy.<sup>10</sup> The assignments are relatively straightforward, based on previous work<sup>6,8–11</sup> and quantum chemical calculations of the vibrational wavenumbers in the  $D_0^+$  state<sup>26</sup> (see Table I). We see the expected dominance of the  $\Delta v = 0$  band, accompanied by other totally symmetric activity, such as the totally symmetric ( $a_g$ ) fundamental bands  $11^1$ ,  $9^1$ ,  $7^1$ ,  $5^1$ , and  $3^1$ . The

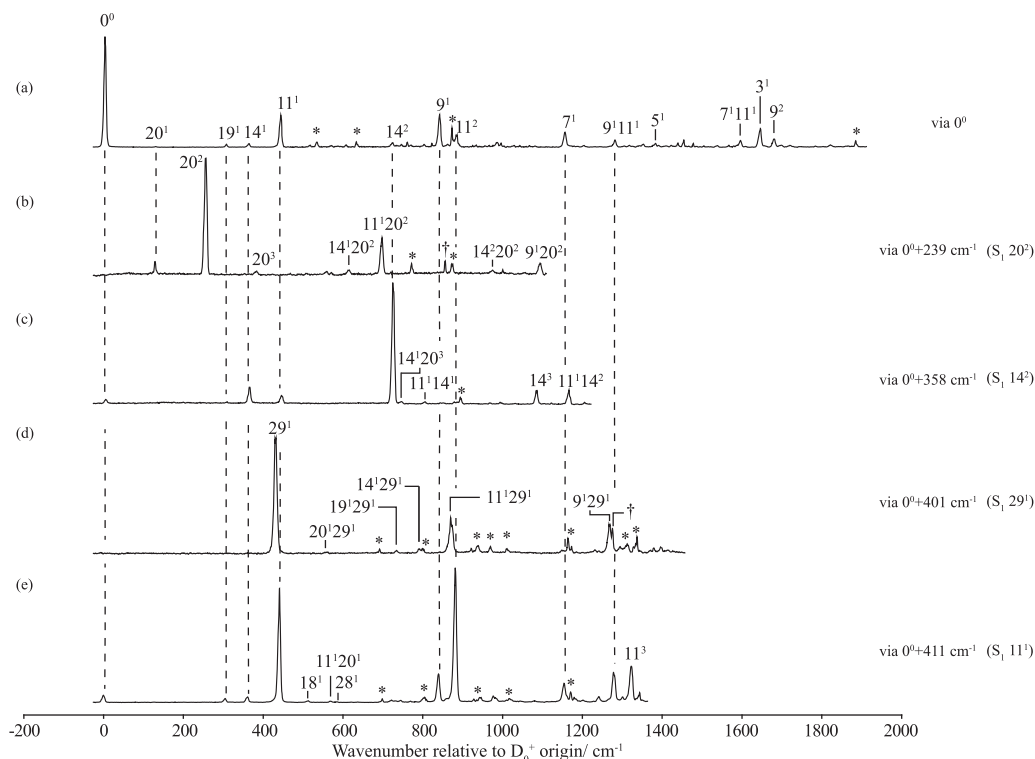


FIG. 2. ZEKE spectra recorded via the indicated  $S_1$  resonances. The indicated intermediate level is assigned as the major contributor—see text for discussion of the assignments. Asterisks and obeli ( $\dagger$ ) indicate accidental resonances and are discussed in Sec. III B.

position of the origin allows the adiabatic ionization energy (AIE) to be determined as  $73\,869 \pm 5\text{ cm}^{-1}$ , which is a little higher than that of Kwon *et al.*<sup>11</sup> ( $73\,861 \pm 5\text{ cm}^{-1}$ ), but in excellent agreement with those of Fujii *et al.*<sup>34</sup> ( $73\,871\text{ cm}^{-1}$ ) and Rieger *et al.*<sup>8</sup> ( $73\,872 \pm 3\text{ cm}^{-1}$ ). Interestingly, to low wavenumber, three non-totally symmetric fundamental bands are observed, corresponding to  $20^1$ ,  $19^1$ , and  $14^1$ , with the terminating levels having  $b_{3u}$ ,  $b_{2g}$ , and  $a_u$  symmetry, respectively. One explanation for their appearance is vibronic coupling<sup>9</sup>—we shall discuss the appearance of these and other such bands in Sec. IV B 2. In other spectra, to be discussed below, it will be seen that many of the assigned bands in Fig. 2(a) appear again, although with different relative intensities; in addition, a number of other bands appear which are not present in the spectrum in Fig. 2(a), showing the utility of recording ZEKE spectra via different intermediate levels.

When recording ZEKE spectra, features arise that are not two-colour in origin and so are not part of the actual  $D_0^+ \leftarrow S_1$  ZEKE spectrum. In Refs. 8 and 9, such signals were attributed to “trapped” electrons, but in recent work on *para*-chlorofluorobenzene (*p*CIFB),<sup>35</sup> we established that a key aspect regarding the appearance of these spurious signals is two-photon, one-colour “accidental resonance” in both the  $S_1$  and  $D_0^+$  states. It was pointed out that the positions of these accidental resonances are coincident with REMPI bands, but the intensities were different—giving an indication of their double resonance character. An accidental resonance signal will be produced if the two-photon energy takes the molecule to high-lying Rydberg states just below an ionization threshold, which are then field-ionized by the pulsed-field extraction, in the usual way as for ZEKE spectroscopy. Alternatively, a signal could also arise when the two-photon energy is just above threshold, if the number of ions present at the laser focus is sufficient to “trap” these slow electrons—this is the suggested mechanism in Refs. 8 and 9. In both cases, we expect a narrow band since the production of the high-lying Rydberg states (or slow electrons) can only occur across a narrow wavenumber range when the laser is also resonant with a  $S_1 \leftarrow S_0$  transition. These one-colour accidental resonance signals appear across the ZEKE spectra and are labeled with an asterisk in each case. Of course, achieving resonance for a second photon being absorbed becomes more likely at higher energies since higher vibrational levels in the cation are being accessed, where the density of states is higher.

A second, but related, two-colour mechanism also occurs. In these cases, the scanning “ionization” laser in the ZEKE experiment becomes resonant with the energy of an  $S_1 \leftarrow S_0$  transition and, additionally, the fixed “excitation” laser is then accidentally resonant with a transition from this  $S_1$  level to a level in the cation. This then leads to the production of high-lying Rydberg states (or perhaps slow electrons), as noted above. These signals are labeled with an obelus ( $\dagger$ ) in the ZEKE spectra, but we refrain from assigning all of these resonances in detail; however, we will comment on several notable ones in the following text—the interested reader can also refer to Ref. 35 to see a discussion of some such resonances in *p*CIFB.

In the present case of *p*DFB, we found that the relative intensities of the accidental resonance bands, particularly the one-colour ones, were very dependent on the day-to-day conditions, although they appeared at the same wavenumbers. This may point to these features being associated more with trapped electrons for *p*DFB, produced just above threshold, than high-lying Rydberg states—in agreement with the suggestion in Refs. 8 and 9.

### C. ZEKE spectra via the overtone features $S_1\ 20^2$ and $S_1\ 14^2$

The ZEKE spectra via the  $20^2$  and  $14^2$  transitions are shown in Figs. 2(b) and 2(c) and are reported here for the first time; each one can be seen to be dominated by the  $\Delta v = 0$  band. Also present in the regions scanned are the  $11^1X^2$  combination bands and, in the case of  $20^2$ , also the  $9^120^2$  combination band. Interestingly, the  $0^0$  and  $11^1$  bands are both reasonably intense in the case of the  $14^2$  spectrum but are absent for  $20^2$ , even though they are Franck-Condon allowed in each case. Via  $S_1\ 14^2$ , we also see two of the symmetry-forbidden bands,  $19^1$  and  $14^1$  (but not  $20^1$ ), that were seen via the origin, but only  $20^1$  is seen when exciting via  $S_1\ 20^2$ , suggesting a different vibronic activity. Notably the strongest non-Franck-Condon bands in each case correspond to  $\Delta v = \pm 1$ .

A weak feature at  $311\text{ cm}^{-1}$  is also seen in the REMPI spectrum that was tentatively assigned to  $14^120^1$  by KK, but we note that this is not consistent with the  $20^2$  and  $14^2$  band positions. KK did not record a DF spectrum. In fact, we are convinced that this REMPI feature is in fact a hot band corresponding to the transition  $11_0^119_1^1$  and is the counterpart of the persistent hot band that appears at  $-100\text{ cm}^{-1}$ , discussed earlier in Sec. III A. We managed to record a weak ZEKE spectrum via this feature consistent with this assignment.

In Ref. 9, a ZEKE spectrum via the  $20^1$  level in  $S_1$  was recorded, accessed via the hot band transition,  $20_1^1$ , providing a wavenumber for  $D_{20}$  in the cation in good agreement with the present value (see Table I) and consistent with the position of the  $20^1$  ZEKE band observed in other spectra reported herein.

The above assignments agree with those of KK.<sup>4</sup>

### D. ZEKE spectra recorded via the fundamentals $S_1\ 29^1$ and $S_1\ 11^1$

These two bands lie close to each other in the REMPI spectrum at  $401\text{ cm}^{-1}$  and  $411\text{ cm}^{-1}$  (see Fig. 1). The vibrations are of different symmetries, being  $b_{3g}$  and  $a_g$ , respectively; the former is vibronically induced by Herzberg-Teller coupling,<sup>4</sup> while the latter is Franck-Condon allowed, although its intensity could also be affected by Herzberg-Teller coupling.<sup>36</sup> The ZEKE spectra obtained are shown in Figs. 2(d) and 2(e). ZEKE spectra via both of these levels were reported in Ref. 9, and our spectra are consistent with those.

The ZEKE spectrum recorded via  $29^1$  may be seen to be dominated by the  $\Delta v = 0$  band, with the expected  $11^129^1$  and  $9^129^1$  combination bands to higher wavenumber, as well as the vibronically induced  $20^129^1$ ,  $19^129^1$ , and  $14^129^1$  bands. The  $0^0$  band is absent in line with Franck-Condon expectations.

On the other hand, the activity in the ZEKE spectrum recorded via  $11^1$  is very different. Immediately apparent is that it is not the  $\Delta\nu = 0$  band, but the  $\Delta\nu = +1$  band,  $11^2$ , that is the most intense, with significant intensities also in  $0^0$  ( $\Delta\nu = -1$ ) and  $11^3$  ( $\Delta\nu = +2$ ). We also see the weak vibronically induced bands  $20^1$  (barely discernible in the figure),  $19^1$ , and  $14^1$ , as well as the  $18^1$  band (not reported in Ref. 9 or 10) and a weak band corresponding to  $28^1$ . There are also a number of other bands corresponding to totally symmetric vibrations, as expected. Overall, it is interesting that these two spectra are mutually exclusive in terms of activity, owing to the difference in the symmetries of the intermediate levels, even though these only lie  $10\text{ cm}^{-1}$  apart.

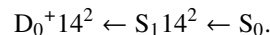
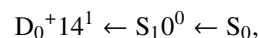
Both of these assignments agree with those of KK.<sup>4</sup>

### E. ZEKE spectra recorded via bands in the region $540\text{--}800\text{ cm}^{-1}$

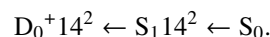
We first discuss three REMPI bands that appear in the lower wavenumber part of this region, at  $545\text{ cm}^{-1}$ ,  $558\text{ cm}^{-1}$ , and  $652\text{ cm}^{-1}$ . ZEKE spectra via each of these features can be seen in Figs. 3(a)–3(c) and are reported here for the first time.

The ZEKE spectrum via the  $545\text{ cm}^{-1}$  level—Fig. 3(a)—is consistent with the assignment of the REMPI band as  $19^2$ , with the  $\Delta\nu = 0$  band at  $613\text{ cm}^{-1}$  in the ZEKE spectrum; this is also consistent with the assignment by KK.<sup>4</sup> There is some similarity of the appearance of the spectrum to that of the  $20^2$  spectrum shown in Fig. 2(b), with the  $\Delta\nu = \pm 1$  bands being seen, as well as the vibronically induced  $14^1 19^2$  band; unfortunately, it was not quite possible to scan as far as the  $0^0$  band with the laser dyes employed. In Ref. 9, a ZEKE spectrum was recorded via the  $19^1$  level, accessed via the hot

band transition,  $19^1_1$ , which gave a value for  $D_{19}$  in the cation in good agreement with the present value (see Table I) and also obtained via other spectra herein. It can be seen that there are two strong two-colour accidental resonances (cf. Sec. III B) in the ZEKE spectrum at  $357\text{ cm}^{-1}$  and  $714\text{ cm}^{-1}$ , which may be assigned, respectively, as



The ZEKE spectrum recorded via the  $558\text{ cm}^{-1}$  level—Fig. 3(b)—shows a strong band at  $584\text{ cm}^{-1}$ , allowing the  $S_1$  level to be assigned to the transition involving the vibronically active  $b_{3g}$  vibration  $D_{28}$ . We also see the expected combination band,  $11^1 28^1$ , to higher wavenumber. The assignment of the  $S_1$  level to  $28^1$  agrees with the assignment of KK,<sup>4</sup> and the ZEKE spectrum firmly establishes the wavenumber for this vibration in both the  $S_1$  and  $D_0^+$  states. A two-colour accidental resonance band (cf. Sec. III B) appears at  $729\text{ cm}^{-1}$ , which corresponds to one of the resonances seen via the  $545\text{ cm}^{-1}$  level, but now at a different apparent wavenumber,



The ZEKE spectrum recorded via the  $652\text{ cm}^{-1}$  feature—Fig. 3(c)—confirms KK's<sup>4</sup> assignment of the  $S_1$  level to  $11^1 20^2$ , with both the  $\Delta\nu = 0$  and  $11^2 20^2$  bands observed. There are several one-colour accidental resonances in this region, plus three two-colour ones (cf. Sec. III B). The latter are at  $861\text{ cm}^{-1}$ ,  $871\text{ cm}^{-1}$ , and  $1017\text{ cm}^{-1}$  and may be assigned, respectively, as

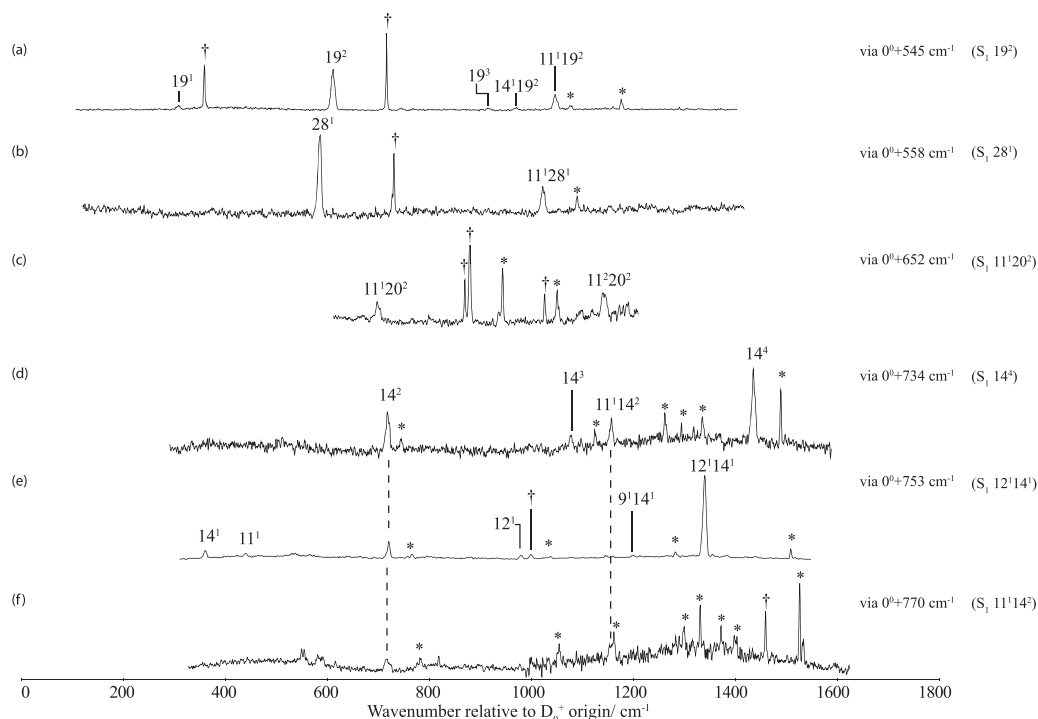
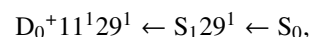
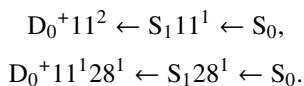


FIG. 3. ZEKE spectra recorded via the indicated  $S_1$  resonances. The indicated intermediate level is assigned as the major contributor—see text for discussion of the assignments. Asterisks and obeli (†) indicate accidental resonances and are discussed in Sec. III B.



We now move onto the REMPI features to higher wavenumber. First, we note that the transition corresponding to the REMPI band at 704  $\text{cm}^{-1}$  was assigned as  $30^2$  by KK<sup>4</sup> on the basis of the  $S_1$  wavenumber of the fundamental from RS,<sup>2</sup> but this was not confirmed by recording DF spectra. The band at 719  $\text{cm}^{-1}$  was unassigned by KK. We have attempted to record ZEKE spectra via both of these features. When exciting via the 704  $\text{cm}^{-1}$  feature, only very weak ZEKE features could be obtained (spectrum not shown), and none of those was at the correct wavenumber for the  $\Delta\nu = 0$  band of  $30^2$ . As such, the assignment of the 704  $\text{cm}^{-1}$  band must remain tentative. When exciting via the 719  $\text{cm}^{-1}$  REMPI band, we did obtain a ZEKE spectrum with reasonable signal-to-noise (not shown); however, it became apparent that the spectrum looked very similar to that obtained via the  $9^1$  REMPI band; hence, this, and its wavenumber, established the assignment of the REMPI feature as a hot band:  $9_0^1 19_1^1$ . (As will be discussed in Sec. III F, the  $D_9$  vibration is in Fermi resonance in the  $S_1$  state and so the notation for this assignment is simplistic.)

Exciting via the band at 734  $\text{cm}^{-1}$  yields a ZEKE spectrum with the most intense band at 1436  $\text{cm}^{-1}$ , being consistent with an assignment to  $14^4$ , also present are the  $14^2$  band at 717  $\text{cm}^{-1}$  and the  $11^1 14^2$  band at 1157  $\text{cm}^{-1}$ —see Fig. 3(d). This assignment is consistent with KK.<sup>4</sup> In  $S_1$ ,  $14^2$  is at 361  $\text{cm}^{-1}$ , and so  $14^4$  being at 734  $\text{cm}^{-1}$  is anomalous (also noted by KK),<sup>4</sup> suggesting a positive anharmonicity; this is plausible since the motion of  $D_{14}$  is ring puckering,<sup>25</sup> which would be pushing atoms closer together.

Exciting via the level at 753  $\text{cm}^{-1}$  yields a ZEKE spectrum with the most intense band at 1339  $\text{cm}^{-1}$ , which may be assigned  $12^1 14^1$ , consistent with both KK<sup>4</sup> and the calculated values—see Fig. 3(e) and Table I. This then identifies a ZEKE band at 980  $\text{cm}^{-1}$  as  $12^1$ , with  $14^1$  also being seen, both consistent with the  $12^1 14^1$  assignment. Also seen in the spectrum are bands due to  $14^2$ ,  $11^1 14^2$ , and  $14^3$ . We also see the  $11^1 14^2$  band in the ZEKE spectrum obtained when exciting via the level at 770  $\text{cm}^{-1}$  (unassigned by KK<sup>4</sup>)—see Fig. 3(f)—and the wavenumber of this intermediate level is consistent with its being  $11^1 14^2$ . There is thus some suggestion that the 753  $\text{cm}^{-1}$  and 770  $\text{cm}^{-1}$   $S_1$  levels arise from Fermi resonance between the  $12^1 14^1$  and  $11^1 14^2$  levels. KK<sup>4</sup> suggested that an LIF band at 789  $\text{cm}^{-1}$  might be  $11^1 14^2$ , but also that this may have arisen from the  $p$ DFB-Ar complex. This would not be at the expected wavenumber for  $11^1 14^2$ , and furthermore, we observed no ZEKE spectrum when exciting at this wavenumber; as a consequence, we reject that assignment.

## F. Fermi resonance in the region 800–830 $\text{cm}^{-1}$

### 1. ZEKE spectra

This region of the REMPI spectrum contains a trio of bands that have been assigned by KK<sup>4</sup> to transitions involving totally symmetric levels:  $29^2$ ,  $9^1$ , and  $11^2$ , with the last two having been assigned as a Fermi resonance in that work, in agreement with CP.<sup>3</sup> The three corresponding REMPI bands are at respective positions of 803  $\text{cm}^{-1}$ , 819  $\text{cm}^{-1}$ , and 822  $\text{cm}^{-1}$ —see Fig. 4. In previous work,<sup>27,37–39</sup> the  $9^1$  and  $29^2$  levels have been assigned as being in Fermi resonance

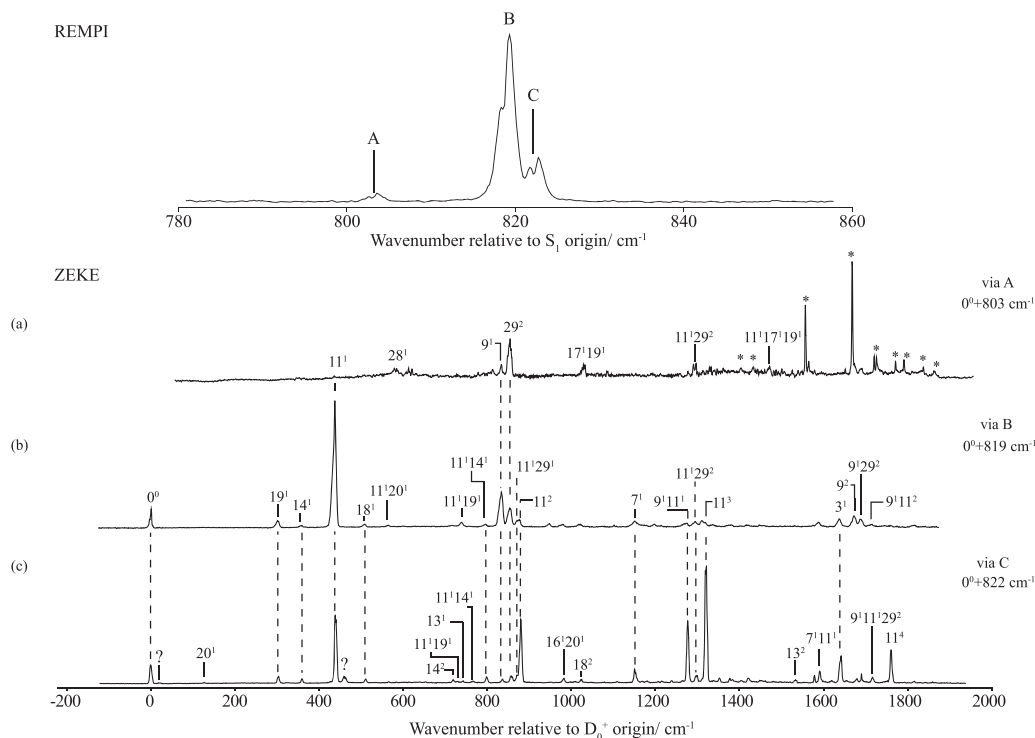


FIG. 4. ZEKE spectra via the  $S_1$   $29^2/9^1/11^2$  Fermi resonance. An expanded view of the 780–860  $\text{cm}^{-1}$  region of the REMPI spectrum shown in Fig. 1 is shown at the top, and the letters indicate the intermediate positions through which the presented ZEKE spectra were recorded. See text for discussion of the assignments. Asterisks and obeli ( $\dagger$ ) indicate accidental resonances and are discussed in Sec. III B.



in *p*F<sub>T</sub>, and this is also the case in *p*CIFB;<sup>29,35</sup> on the other hand, the 29<sup>2</sup> level in *p*Xyl, where it is more energetically removed from the 9<sup>1</sup> level, is at best exceptionally weak.<sup>39</sup> We have taken these observations to imply that the 29<sup>2</sup> transition is only active in the S<sub>1</sub> ← S<sub>0</sub> transition of these disubstituted benzenes by virtue of Fermi resonance, with its activity determined by how energetically proximate the 9<sup>1</sup> and 29<sup>2</sup> levels are.<sup>39</sup> In the present case of *p*DFB, the separation of these two levels is between that of *p*Xyl and that of both *p*F<sub>T</sub> and *p*CIFB, and as such, we might expect the appearance of 29<sup>2</sup> also to be attributable to Fermi resonance. We thus recorded ZEKE spectra via these three intermediate levels, and these are presented in Figs. 4(a)–4(c), which also shows an expanded view of the relevant region of the REMPI spectrum. (Note that we have presented a preliminary discussion of these spectra<sup>39</sup> when comparing between four *para*-disubstituted benzenes.)

The ZEKE spectrum recorded via the band at 803 cm<sup>-1</sup> is shown in Fig. 4(a) and demonstrates the most intense band at 857 cm<sup>-1</sup>, which can be straightforwardly assigned to 29<sup>2</sup>. There are weak bands due to 28<sup>1</sup>, 9<sup>1</sup>, and 11<sup>1</sup>29<sup>2</sup>. The weak appearance of 9<sup>1</sup> is consistent with a Fermi resonance interaction: 9<sup>1</sup>...29<sup>2</sup>; note that we see no significant 11<sup>2</sup> band. Of interest is a band at 1035 cm<sup>-1</sup>, whose assignment to the 17<sup>1</sup>19<sup>1</sup> Δ<sub>v</sub> = 0 band follows from the suggestion by KK<sup>4</sup> of the intermediate feature being the overlap of two bands; additionally, the 11<sup>1</sup>17<sup>1</sup>19<sup>1</sup> band may be seen at 1475 cm<sup>-1</sup>. This assignment yields values for the D<sub>17</sub> vibration in the S<sub>1</sub> and D<sub>0</sub><sup>+</sup> states of 529 cm<sup>-1</sup> and 730 cm<sup>-1</sup>, respectively, which fit well with the calculated values (see Table I). The derived S<sub>1</sub> value for D<sub>17</sub> fits the calculated trends, namely, that the experimental values lie below the calculated ones.

We now move on to considering the ZEKE spectra obtained when exciting via the bands at 819 and 822 cm<sup>-1</sup>—see Figs. 4(b) and 4(c). These bands were concluded to arise from a Fermi resonance pair, arising from a 11<sup>2</sup>...9<sup>1</sup> interaction by CP<sup>3</sup> and this was agreed with by KK.<sup>4</sup> We now examine whether the ZEKE spectra confirm this. First, the spectrum obtained when exciting via the 822 cm<sup>-1</sup> feature—Fig. 4(c)—shows a progression in the D<sub>11</sub> mode, with an intensity maximum for 11<sup>3</sup>; this activity is in line with the most intense band in the ZEKE spectrum being for 11<sup>2</sup> when exciting via the 11<sup>1</sup> intermediate level—see Fig. 2(e). The profile is unusual in that the 11<sup>1</sup> ZEKE band is more intense than might be expected from the profile inferred from the other members of the progression. We note that the 9<sup>1</sup> ZEKE band is somewhat weak in this spectrum, and there is also a weak band arising from 29<sup>2</sup>. When we examine the 800–900 cm<sup>-1</sup> region of the ZEKE spectrum obtained when exciting via the 819 cm<sup>-1</sup> feature—Fig. 4(b)—we see a very different picture: now the 9<sup>1</sup> band is locally the most intense, but with the 29<sup>2</sup> and 11<sup>2</sup> ZEKE bands being clearly seen. (The 29<sup>2</sup> band was seen in the two-colour MATI study,<sup>10</sup> with 29<sup>2</sup> being one of the three possible assignments offered.) Of great prominence is the intensity of the 11<sup>1</sup> band, which is by far the most intense band in the spectrum; even if the intensities of the 0<sup>0</sup>, 9<sup>1</sup>, and 9<sup>2</sup> bands are summed, this would still be less than the intensity of the 11<sup>1</sup> band. This abnormally intense 11<sup>1</sup> band is also seen

in the two-colour MATI study of Ref. 10, as well as in the REMPI-PES spectra of Sekreta *et al.*<sup>6</sup> and Bellm and Reid.<sup>7</sup> This unusual activity of the D<sub>11</sub> vibration was also commented in the DF studies of CP<sup>3</sup> and KK<sup>4</sup> and attributed to the Fermi resonance.

A weak ZEKE band at 462 cm<sup>-1</sup> may be seen in Fig. 4(c) and is marked with ?, whose assignment is uncertain, but seems to be the 11<sup>1</sup> counterpart of the weak band at 22 cm<sup>-1</sup> (also marked with ?) that is seen close to the origin in the same spectrum; both of these bands were seen in the MATI study of Lembach and Brutschy,<sup>10</sup> where they were also unassigned.

In conclusion, we assign the three S<sub>1</sub> levels at 803 cm<sup>-1</sup>, 819 cm<sup>-1</sup>, and 822 cm<sup>-1</sup>, respectively, to the following, where the leading term indicates the majority contribution and the ... indicate Fermi resonance,

$$\begin{aligned} &29^2 \dots 9^1 \dots 11^2, \\ &9^1 \dots 29^2 \dots 11^2, \\ &11^2 \dots 9^1 \dots 29^2. \end{aligned}$$

Interactions with the 29<sup>2</sup> level appear to be weak since the S<sub>1</sub> fundamental is at 401 cm<sup>-1</sup>, and the overtone is close to the expected position, at 803 cm<sup>-1</sup>, assuming small anharmonicity. This also seems to be the case for the 11<sup>2</sup> level since the 11<sup>1</sup> band is at 411 cm<sup>-1</sup> and the overtone is at 822 cm<sup>-1</sup>. This picture is slightly complicated since the overtones may be expected to lie lower in wavenumber as the result of (diagonal) anharmonicity, and so their actual positions will be a combination of anharmonicity and Fermi resonance. Even so, in both cases, the energetic shifts appear to be small.

## 2. Time-resolved photoelectron spectra

In Fig. 5(a), we show two overlaid photoelectron spectra recorded using 1 ps laser pulses for the pump and probe. These spectra were recorded with pump-probe time delays of 0 ps and 5 ps and clearly show the differing intensities of the photoelectron bands. In particular, the 0<sup>0</sup> band is strongest in the 0 ps spectrum and the 11<sup>1</sup> band is strongest in the spectrum recorded with a delay of 5 ps. The time-dependent intensity of the 0<sup>0</sup> band can be determined by scanning the delay stage; the result of this is plotted in Fig. 6(a). (For time delays <2 ps, the relative intensities are less reliable owing to strong field effects when the excitation and ionization laser beams are overlapped temporally.) A Fourier transform of the data in Fig. 6(a) is shown in Fig. 6(b), where two clear peaks may be seen at 3.6 cm<sup>-1</sup> and 7.2 cm<sup>-1</sup>; these features correspond to angular frequencies of 0.68 and 1.37 rad s<sup>-1</sup> and oscillation periods of 9.2 and 4.6 ps, respectively. The peaks in the Fourier transform in Fig. 6(b) correspond to the separation of the contributing vibrational eigenstates.

The angular frequencies from the Fourier transform were used as initial values in the following empirical equation for the time-dependence of the data in Fig. 6(a):

$$C_a \cos(\omega_a t) + C_b \cos(\omega_b t) + C_c, \quad (1)$$

where the ω<sub>*i*</sub> are the angular frequencies. Least-squares fitting to the time profile shown in Fig. 6(a) led to very slightly refined

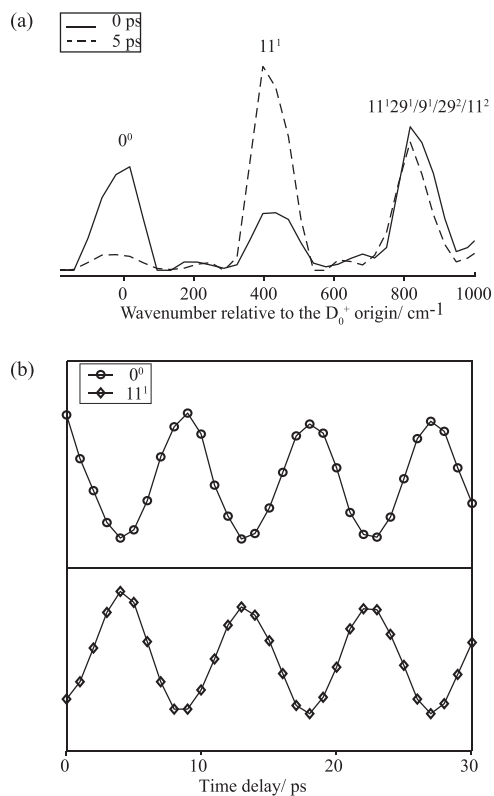


FIG. 5. (a) Photoelectron spectrum recorded following the coherent excitation of the  $9^1 \dots 11^2 \dots 29^2$  and  $11^2 \dots 9^1 \dots 29^2$  eigenstates using ps laser pulses. The spectrum is shown at two time delays: the solid line denotes the spectrum recorded at a delay between the pump and probe pulses of 0 ps, while the dashed line denotes the spectrum recorded at 5 ps. The resolution is  $\sim 200 \text{ cm}^{-1}$  and consequently a number of transitions may contribute to a feature—compare with the ZEKE spectra in Fig. 4. (b) Time variation of the  $0^0$  and  $11^1$  photoelectron bands as a function of the time delay between the excitation and ionization pulses following the coherent excitation of the  $9^1 \dots 11^2 \dots 29^2$  and  $11^2 \dots 9^1 \dots 29^2$  eigenstates using the ps laser pulses. The symbols indicate photoelectron intensities determined from the area of the relevant photoelectron band, while the lines are just to guide the eye.

values of the  $\omega_i$ , giving wavenumber separations of the eigenstates as  $3.6 \text{ cm}^{-1}$  and  $7.3 \text{ cm}^{-1}$  and corresponding to periods of 9.2 ps and 4.6 ps, respectively. The fit to Eq. (1) is robust—see Fig. 6(a)—with  $R^2 = 0.96$ .

From the discussion of the ZEKE results above, and from the results of other studies by CP<sup>3</sup> and KK,<sup>4</sup> we expect the  $9^1$  and  $11^2$  levels to be interacting. The deduced eigenstate spacing of  $3.6 \text{ cm}^{-1}$  is in excellent agreement with the REMPI spacing of  $3.5 \text{ cm}^{-1}$  between bands B and C in Fig. 4, confirming this interaction. The other spacing of  $7.2 \text{ cm}^{-1}$  indicates the presence of a third state. The bandwidth ( $13 \text{ cm}^{-1}$ ) of the picosecond laser pulse was too narrow to encompass the  $29^2 \dots$  Fermi resonance component coherently with the other two eigenstates (see Fig. 4), and so the 0 ps photoelectron spectrum in Fig. 5(a) will not be completely indicative of the zero-order bright state, although it will contain a  $29^2$  contribution by virtue of its presence in the  $9^1 \dots$  and  $11^2 \dots$  eigenstates. The  $\sim 200 \text{ cm}^{-1}$  resolution of the photoelectron spectrum was not sufficient to resolve the  $9^1$ ,  $29^2$ , and  $11^2$  bands, which all lie under the third photoelectron band at  $\sim 850 \text{ cm}^{-1}$  in Fig. 5(a).

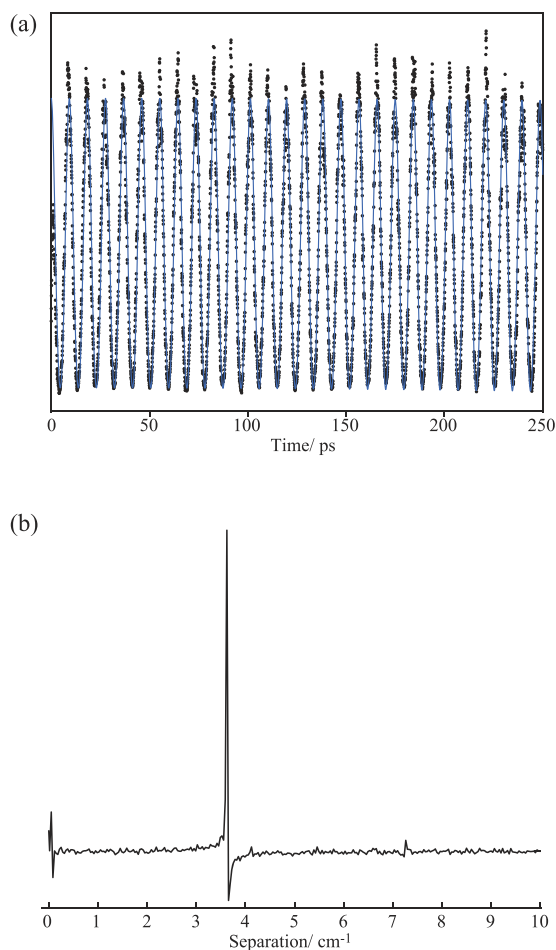


FIG. 6. (a) Variation of the intensity of the  $0^0$  band as a function of the time delay between the excitation and ionization lasers, following the coherent excitation of the  $9^1 \dots 11^2 \dots 29^2$  and  $11^2 \dots 9^1 \dots 29^2$  eigenstates using ps laser pulses. The dots are experimental intensities obtained by scanning the delay stage, and the solid line is a fit to the empirical data—see text for details. (b) Fourier transform of the empirical data shown in (a). The two peaks observed correspond to energy separations between eigenstates—see text for further details.

Looking at the possible totally symmetric levels that may be interacting, the only viable candidate for the third state is the  $14^1 19^1 30^1$  level. However, this is expected to appear at a lower wavenumber in the  $S_1$  state and to result in a ZEKE band at  $1033 \text{ cm}^{-1}$ . No such band is observed and so this hypothesis is discarded. Because there are no other totally symmetric levels, we looked for levels of  $b_{3g}$  symmetry. A likely candidate is the  $11^1 29^1$  level which could potentially couple via Coriolis coupling; however, this has a reduced likelihood under jet-cooled conditions, and so we suggest Herzberg-Teller coupling as the more likely possibility. This mechanism has previously been invoked in the  $S_1$  state (see Sec. IV B 1) and is reminiscent of a related coupling seen in pFT between vibration-torsion (vibtor) levels.<sup>40</sup> There is a weak shoulder to the most intense REMPI band at  $\sim 820 \text{ cm}^{-1}$ , which may be seen in the inset of Fig. 1, and this matches the expected position for  $11^1 29^1$ . Furthermore, in the ZEKE spectra reported in Fig. 4, which were recorded via the two most intense REMPI bands, we see a weak band at  $870 \text{ cm}^{-1}$ , which also fits the expected position

of the  $\Delta v = 0$  band for the  $11^1 29^1$  transition. Hence, there is some evidence from the ZEKE spectra presented above to support the involvement of  $11^1 29^1$  in the Fermi resonance in  $S_1$ . The evidence, such as the weak feature seen in the Fourier transform—Fig. 6(b)—suggests that the interaction is weak.

In Fig. 5(b), we show the time dependence of two of the cleanest contributions to the photoelectron spectra shown in Fig. 5(a); these correspond to the  $0^0$  and  $11^1$  bands. These were determined by fitting the photoelectron peaks to Gaussian functions and then plotting the Gaussian areas as a function of time delay. The resulting intensity variations of the two bands are rather interesting. The behavior of the  $0^0$  contribution is consistent with its being associated with the zero-order bright state, having maximum intensity at  $t = 0$  ps. By contrast, the  $11^1$  band is out of phase, consistent with its being associated with a dark state, although its intensity does not drop to zero at any point. We interpret this in terms of there being non-zero Franck-Condon factors (FCFs) between each of the  $9^1$  and  $11^2$  zero-order states and  $11^1$  in the cation, but it is also possible that the  $11^2$  zero-order state has a small amount of brightness, which would be consistent with other related molecules.<sup>39</sup> This unusual behavior of the  $11^1$  band complicates the interpretation of the time-dependent behavior and is consistent with suggestions from CP<sup>3</sup> and KK.<sup>4</sup> The inference from Fig. 5(b) is that the majority contribution to the  $11^1$  photoelectron band comes from  $S_1$   $11^2$ , consistent with  $9^1$  being the zero-order bright state and  $11^2$  being the zero-order dark state. This picture is reminiscent of the behavior seen for *p*FT when exciting via the  $9^1$  and  $11^2$

levels,<sup>27</sup> although in that case the  $9^1$  level is interacting with  $29^2$  in *p*FT, and  $11^2$  overlaps with  $12^1 14^1$ . With this in mind, we look back at the ZEKE spectra in Figs. 4(b) and 4(c), which indicate that band B in the REMPI spectrum in Fig. 4 is dominated by  $9^1$ , while band C is dominated by  $11^2$ . It is somewhat surprising that the  $11^1$  band is so intense in Fig. 4(b), and in their fluorescence study, KK<sup>4</sup> suggested that there are transition moment interference effects for these levels.

The third, highest wavenumber feature in Fig. 5(a), required at least three Gaussian functions in order to model the photoelectron band profile at all times, consistent with the underlying  $11^1 29^1$ ,  $9^1$ ,  $11^2$ , and  $29^2$  bands discussed above. Because these overlap strongly, it was not possible to perform a confident deconvolution of their time-dependence at this resolution.

### G. ZEKE spectra recorded via bands in the range 880–960 $\text{cm}^{-1}$

An expanded view of this region of the REMPI spectrum is shown in Fig. 7, and the ZEKE spectrum recorded via  $0^0 + 880 \text{ cm}^{-1}$  is shown in Fig. 7(a). The intermediate level has been assigned<sup>4</sup> as  $S_1$   $18^2$ , consistent with the strong  $\Delta v = 0$  ZEKE band at  $1023 \text{ cm}^{-1}$ , allowing a value for  $D_{18}$  in the cation of  $512 \text{ cm}^{-1}$  to be established. The expected  $11^1 18^2$  and  $9^1 18^2$  bands may be seen to higher wavenumber, and the vibronically induced  $18^2 19^1$  and  $14^1 18^2$  bands are also present. Although the  $18^1$  band appears to be too weak to observe, we do see the vibronically induced  $18^3$  band.

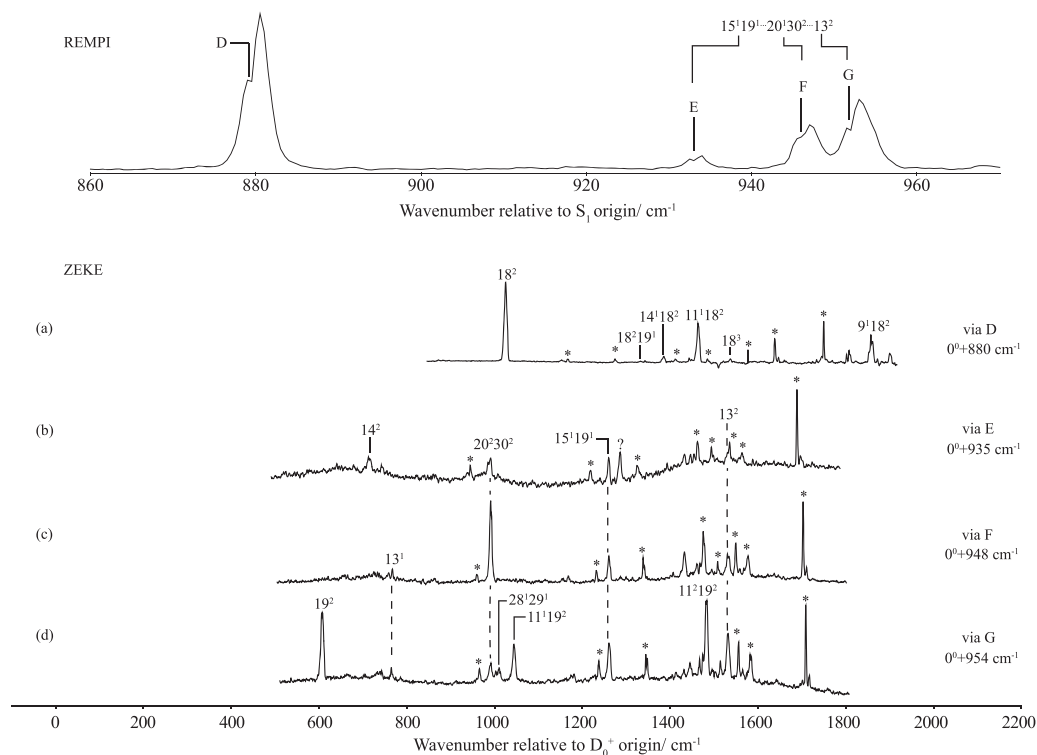


FIG. 7. An expanded view of the  $860\text{--}970 \text{ cm}^{-1}$  region of the REMPI spectrum shown in Fig. 1 is shown at the top. ZEKE spectra recorded via the  $S_1$   $18^2$  resonance is shown in (a), while traces (b)–(d) show ZEKE spectra recorded at the positions indicated by letters on the REMPI trace. See text for discussion of the assignments. Asterisks and obeli ( $\dagger$ ) indicate accidental resonances and are discussed in Sec. III B.

There are three other REMPI bands in this region, at  $935\text{ cm}^{-1}$ ,  $948\text{ cm}^{-1}$ , and  $954\text{ cm}^{-1}$ . The ZEKE spectra recorded via these levels form an interesting group, with a number of common bands that appear in all three spectra. Common bands (and their assignments) are  $991\text{ cm}^{-1}$  ( $20^230^2$ ),  $1260\text{ cm}^{-1}$  ( $15^119^1$ ), and  $1530\text{ cm}^{-1}$  ( $13^2$ ). The strong ZEKE band at  $991\text{ cm}^{-1}$  when exciting via  $0^0 + 948\text{ cm}^{-1}$  and the strong  $19^2$ ,  $11^119^2$ , and  $11^219^2$  bands when exciting via  $0^0 + 954\text{ cm}^{-1}$  indicate that significant contributing levels to these two bands are  $20^230^2$  and  $11^119^2$ , respectively, in agreement with the assignments by KK.<sup>4</sup> KK also suggested that  $13^2$  may be involved in these two levels and it appears to have its largest relative intensity when exciting at  $0^0 + 954\text{ cm}^{-1}$ . Since the contributions from the  $20^230^2$ ,  $15^119^1$ , and  $13^2$  levels appear across all three spectra, this supports the fact that they are all involved in a complex Fermi resonance. (A band assignable as  $13^1$  is seen when exciting at  $0^0 + 948$  and  $0^0 + 954\text{ cm}^{-1}$ .)

On the other hand, a ZEKE band at  $1286\text{ cm}^{-1}$  is seen only when exciting via  $0^0 + 935\text{ cm}^{-1}$  suggesting that this may be an overlapped feature. Although the assignment of KK to  $26^1$  fits both their DF spectra, and indeed the band in the ZEKE spectrum in Fig. 7(b) according to the calculated cationic value (see Table I), the  $S_1$  calculated value is far removed from the excitation position, and so we are not happy with this assignment. We have no alternative assignment at the present time, and so leave the corresponding ZEKE feature unassigned—marked with ? in Fig. 7(b).

A weak ZEKE band is seen at  $1011\text{ cm}^{-1}$  when exciting via the  $954\text{ cm}^{-1}$  intermediate level, and this is a good fit to being a  $\Delta\nu = 0$  band for  $28^129^1$ , which is also expected at this wavenumber.

In summary, we assign this trio of bands to the following, where the leading term of the Fermi resonance indicates the majority contribution,

$$\begin{aligned} 935\text{ cm}^{-1} &: 15^119^1 \dots 13^2 \dots 20^230^2 + \text{an unknown overlapped feature,} \\ 948\text{ cm}^{-1} &: 20^230^2 \dots 13^2 \dots 15^119^1, \\ 954\text{ cm}^{-1} &: 13^2 \dots 15^119^1 \dots 20^230^2 + \text{overlapped } 11^119^2 \text{ and } 28^129^1. \end{aligned}$$

Thus, these are a rather complicated set of bands, and rather intriguing since the  $20^230^2$ ,  $15^119^1$ , and  $13^2$  pervade the spectra, even though the  $935\text{ cm}^{-1}$  band is more separated than the other two bands. In addition, two of the bands have extra contributions from overlapped features.

The assignment of these bands allows the values of the following vibrational wavenumbers to be deduced in the  $S_1$  and  $D_0^+$  states, respectively, albeit acknowledging that there may be shifts from the Fermi resonance interactions:  $D_{13}$  as  $477\text{ cm}^{-1}$  and  $765\text{ cm}^{-1}$ ,  $D_{15}$  as  $660\text{ cm}^{-1}$  and  $955\text{ cm}^{-1}$ , and  $D_{30}$  as  $355\text{ cm}^{-1}$  (consistent with  $RS^2$ ) and  $369\text{ cm}^{-1}$ .

## H. Feature at $1059\text{ cm}^{-1}$

An expanded view of this REMPI feature is shown in Fig. 8, and it appears to have more than one contribution. KK<sup>4</sup> concluded that there were two bands: at  $1057\text{ cm}^{-1}$  (lower-wavenumber shoulder) and  $1058\text{ cm}^{-1}$  (main band). They assigned the main band to  $9^120^2$  and the shoulder to  $16^118^1$  with possible contributions from  $17^2$  and  $9^120^2$ . We present two ZEKE spectra recorded via this feature, which are shown in Figs. 8(a) and 8(b).

We consider first the ZEKE spectrum obtained via the dip in the more intense part of the band, which is shown in Fig. 8(a). We can see that there are a number of strong ZEKE bands, and one of those at a higher-wavenumber is consistent with being the  $17^2$  band at  $1453\text{ cm}^{-1}$ , and we assign this as the  $\Delta\nu = 0$  band, consistent with the  $D_{17}$  cation value derived in Sec. III F. The band next to it at  $1461\text{ cm}^{-1}$  may be assigned to  $14^117^130^1$ , which is totally symmetric. If we then

consider the DF study by KK,<sup>4</sup> then we see that the expected  $S_0$  position of this latter level is  $1462\text{ cm}^{-1}$ , while for  $16^118^1$  it would be  $1343\text{ cm}^{-1}$ ; thus, the unassigned  $1470\text{ cm}^{-1}$  DF band seen by KK<sup>4</sup> nicely fits the  $14^117^130^1$  assignment, and while the  $1343\text{ cm}^{-1}$  DF band would be consistent with the  $16^118^1$  assignment of KK, in the cation  $16^118^1$  would be at  $1357\text{ cm}^{-1}$ , and there is no clear ZEKE band at that position; of course, the activity in the two transitions might not necessarily be the same.

When exciting via the level dominated by  $9^1$  (Sec. III F), unusual Franck-Condon factors were apparent, leading to the  $11^1$  band being the most intense, with also intensity in the  $29^2$  and  $11^2$  bands. We can see that this behavior is consistent with a contribution from  $9^120^2$  to the ZEKE spectrum in Fig. 8(a), with an intense band at  $694\text{ cm}^{-1}$  ( $11^120^2$ ) and the  $\Delta\nu = 0$  band,  $9^120^2$  at  $1089\text{ cm}^{-1}$  being much less intense; in addition, there is the close-lying  $20^229^2$  band, being of similar intensity. By contrast, the ZEKE spectrum in Fig. 8(b) suggests that the  $17^2$  band dominates the eigenstate at  $1060\text{ cm}^{-1}$ . Overall, these two spectra suggest that the low-wavenumber side of the REMPI band arises from  $9^120^2$ , with perhaps some overlap/Fermi resonance with the main  $17^2$  band. The  $14^117^130^1$  band is most prominent when exciting on the low wavenumber side of the feature. The Fermi resonance behavior within this REMPI feature is a little unclear, particularly as there is an accidental resonance coincident with the  $17^2$  feature. It appears reasonable to assume that the  $14^117^130^1$  activity results from Fermi resonance with  $17^2$ , with the former feature appearing as a shoulder in Fig. 8(b). The absence of the  $11^120^2$  and  $9^120^2$  bands in the latter spectrum

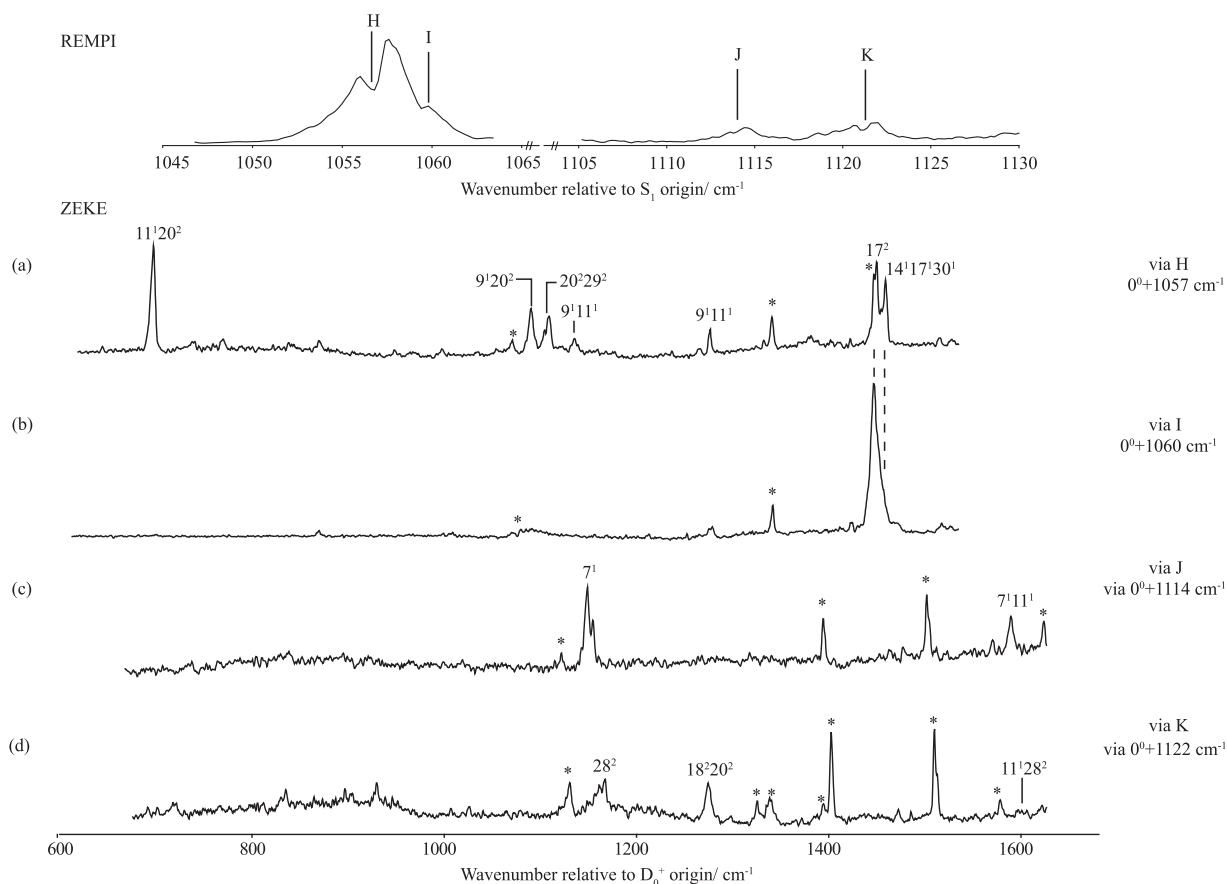


FIG. 8. An expanded view of the 1047–1063  $\text{cm}^{-1}$  and 1105–1130  $\text{cm}^{-1}$  regions of the REMPI spectrum shown in Fig. 1 is presented at the top showing the bands that are used as intermediates in recording the ZEKE spectra presented. The letters on the REMPI trace indicate the intermediate positions through which the presented ZEKE spectra were recorded. See text for discussion of the assignments. Asterisks and obeli ( $\dagger$ ) indicate accidental resonances and are discussed in Sec. III B.

suggests that no Fermi resonance is occurring between  $9^1 20^2$  and  $17^2$ .

This assignment to  $9^1 20^2$  would also lead us to expect to see a REMPI band arising from  $11^2 20^2$  (owing to the  $29^2/9^1/11^2$  Fermi resonance); however, when we excite to slightly higher wavenumber, we only see a broadened feature around 1100  $\text{cm}^{-1}$  in Fig. 8(b), and no  $11^2 20^2$  band. (We also attempted to record ZEKE spectra on the far wings of the REMPI feature shown at the top of Fig. 8, but we only saw clear features from accidental resonances in those cases.)

### I. Bands in the range 1110–1140 $\text{cm}^{-1}$

There are three bands here, although KK<sup>4</sup> only mentioned one, at 1116  $\text{cm}^{-1}$ , which they say consists of overlap/Fermi resonance with five features:  $12^1 14^3$ ,  $14^6$ ,  $28^2$ ,  $18^2 20^2$ , and  $7^1$ . When we excite via the 1114  $\text{cm}^{-1}$  feature, we see a clean spectrum assignable to  $7^1$ , with the  $7^1 11^1$  band also present—see Fig. 8(c). When we excite at 1122  $\text{cm}^{-1}$ , Fig. 8(d), we see a spectrum that consists of two ZEKE bands: a band at 1168  $\text{cm}^{-1}$ , which can be straightforwardly assigned to  $28^2$ ; and a band at 1275  $\text{cm}^{-1}$  which may be assigned to  $18^2 20^2$ , which fits both the  $S_1$  and ZEKE band wavenumbers. Thus, this REMPI feature comprises two overlapped bands.

A weak REMPI band is also observed at 1130  $\text{cm}^{-1}$  from which a very weak ZEKE spectrum was obtained. The ZEKE band positions were not consistent with the REMPI band being a cold feature, and indeed we assign this REMPI feature to a hot band corresponding to  $9^1_0 11^1_0 19^1_1$ .

### J. Bands in the range 1150–1195 $\text{cm}^{-1}$

There are six REMPI bands in this region, an expanded version of which is shown at the top of Fig. 9.

We were able to record a ZEKE spectrum when exciting at  $0^0 + 1154 \text{ cm}^{-1}$ , but the excitation wavenumber and the appearance of the spectrum confirmed that this REMPI band is a hot feature, assigned as  $5^1_0 19^1_1$ .

The ZEKE spectrum when exciting at  $0^0 + 1165 \text{ cm}^{-1}$ —Fig. 9(a)—can straightforwardly be assigned as predominantly  $11^1 12^1 14^1$ , with the most intense bands being the  $\Delta v = -1$  band at 1339  $\text{cm}^{-1}$  and the  $\Delta v = 0$  band at 1776  $\text{cm}^{-1}$ . We also see clear  $11^1 14^1$  and  $12^1$  component bands at 797  $\text{cm}^{-1}$  and 980  $\text{cm}^{-1}$ , and some other weak totally symmetric bands (and associated vibronic bands). To higher wavenumber, a band at 1957  $\text{cm}^{-1}$  may be seen and can be assigned to  $12^2$ .

The ZEKE spectrum recorded via  $0^0 + 1170 \text{ cm}^{-1}$ , shown in Fig. 9(b), may be seen to have a sizeable  $12^2$  band,

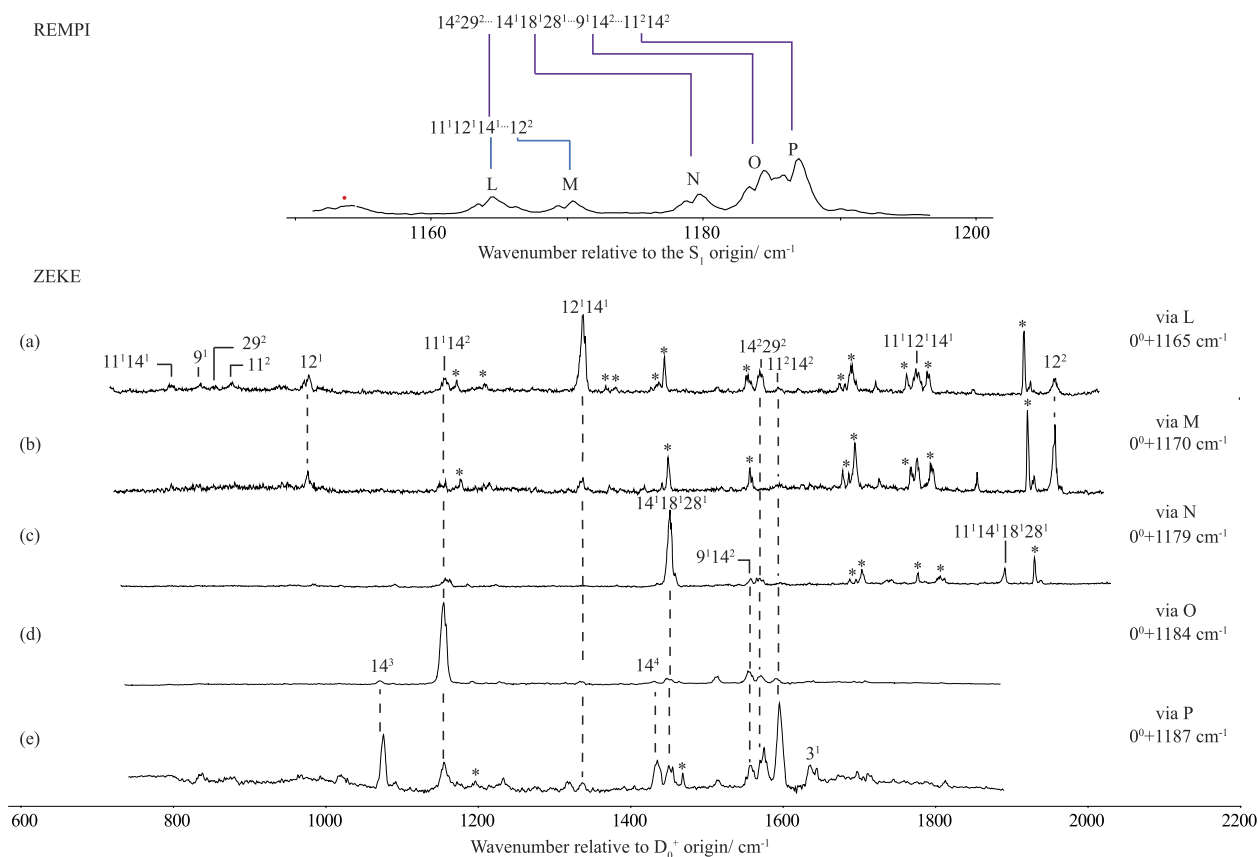


FIG. 9. An expanded view of the 1150–1195  $\text{cm}^{-1}$  region of the REMPI spectrum shown in Fig. 1 is presented at the top showing the bands that are used as intermediates in recording the ZEKE spectra presented. See text for discussion of the assignments. The REMPI band at 1155  $\text{cm}^{-1}$  is a hot band and indicated by a red dot.

suggesting that this is the major contributor to the intermediate level, but there is still significant intensity from the bands associated with  $11^1 12^1 14^1$ . It is clear that the assignment of the 1165  $\text{cm}^{-1}$  and 1170  $\text{cm}^{-1}$  bands is to a Fermi resonance pair,  $11^1 12^1 14^1 \dots 12^2$  and  $12^2 \dots 11^1 12^1 14^1$ , respectively. Interestingly, we also see the  $14^2 29^2$  band at 1572  $\text{cm}^{-1}$  in Fig. 9(a), which will be commented further in the next paragraphs.

When we excite at  $0^0 + 1179 \text{ cm}^{-1}$ , a very different ZEKE spectrum—Fig. 9(c)—emerges that is dominated by the 1453  $\text{cm}^{-1}$  band. Although this is very close to the wavenumber for the  $17^2$  band, that feature was a  $\Delta v = 0$  band when exciting via the 1059  $\text{cm}^{-1}$  feature (Sec. III H), yet this does look very much like a  $\Delta v = 0$  band here. In addition, the expected  $S_0$  value would be at 1380  $\text{cm}^{-1}$  for  $17^2$ , and there is no prominent band in the DF spectra when exciting via this feature,<sup>4</sup> and so we searched for an alternative assignment. The only totally symmetric combination band that appears to fit the  $S_1$  excitation position and the ZEKE band wavenumber is  $14^1 18^1 28^1$ . This assignment would lead to an expectation of a DF band at  $\sim 1560 \text{ cm}^{-1}$ , and indeed a band is seen at 1580  $\text{cm}^{-1}$ ,<sup>4</sup> making this assignment, also suggested by KK, plausible. The band may be gaining intensity via interactions with the surrounding combinations that involve  $14^2$ , as well as the  $11^1 12^1 14^1$  transition.

We note that Reiser *et al.*<sup>9</sup> assigned the 1179  $\text{cm}^{-1}$  intermediate to the  $13^2$  level in their ZEKE study, which was an

uncertain assignment put forward by KK,<sup>4</sup> however, KK also suggested the activity of  $13^2$  when recording DF spectra from bands at  $\sim 950 \text{ cm}^{-1}$  (see Sec. III G). It would be unusual for Fermi resonance to occur over a range of  $>100 \text{ cm}^{-1}$ , and as we have commented above, the presence of  $13^2$  activity suggests involvement in a complex Fermi resonance involving two other levels in the 930–955  $\text{cm}^{-1}$  region. Hence, we conclude that previous assignments of this feature<sup>4,9</sup> to  $13^2$  are incorrect.

There are other bands that are expected in this wavenumber region and, in particular, the  $9^1 14^2$ ,  $14^2 29^2$ , and  $11^2 14^2$  bands, which correspond to combinations of  $14^2$  with each of the Fermi resonance triplets at 800–825  $\text{cm}^{-1}$ , and we now discuss the assignment of these.

We have already pointed out the presence of the  $14^2 29^2$  ZEKE band when exciting at 1165  $\text{cm}^{-1}$ —Fig. 9(a). Exciting at  $0^0 + 1184 \text{ cm}^{-1}$  gives the ZEKE spectrum shown in Fig. 9(d), with a band at 1596  $\text{cm}^{-1}$  that can be assigned as  $11^2 14^2$ . There is also evidence of a small contribution from  $9^1 14^2$  at 1558  $\text{cm}^{-1}$ , which gives the expected more intense  $11^1 14^2$  band at 1156  $\text{cm}^{-1}$ . Thus, the source of these bands can be assigned as a level dominated by the  $S_1$   $9^1 14^2$  level, with the intensities of the corresponding bands being similar to those for  $9^1 \dots$ —see Fig. 4(b); this includes the  $14^2 29^2$  band. There is also a weak  $14^1 18^1 28^1$  band.

When exciting at 1187  $\text{cm}^{-1}$ , we assign the most intense band in the ZEKE spectrum in Fig. 9(e) as  $11^2 14^2$ , which is the

$\Delta\nu = 0$  band. Associated with this, cf. the  $14^2$  and  $11^2 \dots$  ZEKE spectra in Figs. 2(c) and 4(c), we see the  $14^2 19^1$ ,  $14^3$ ,  $11^1 14^2$ ,  $9^1 14^2$ ,  $14^2 29^2$ , and  $14^4$  bands. In addition, we see a sizeable  $14^1 18^1 28^1$  band. The intermediate level is thus assigned as a level dominated by  $11^2 14^2$ .

The activity above suggests that the  $1165 \text{ cm}^{-1}$ ,  $1184 \text{ cm}^{-1}$ , and  $1187 \text{ cm}^{-1}$  features comprise a complex Fermi resonance made up of bands corresponding to  $14^2$  in combination with the  $(29^2/9^1/11^2)$  Fermi resonance levels, with the overall activity being very similar to that seen in the spectra presented in Fig. 4. This is complicated by contributions from the  $14^1 18^1 28^1$  level to the  $14^2 + (29^2/9^1/11^2)$  complex resonance, with a dominant contribution to the  $1179 \text{ cm}^{-1}$  band. In addition, overlapping this is a separate Fermi resonance involving the  $11^1 12^1 14^1$  and  $12^2$  levels, with the lower one overlapping the Fermi resonance level dominated by  $14^2 29^2$ —see the top of Fig. 9.

A very weak ZEKE spectrum was recorded via  $0^0 + 1191 \text{ cm}^{-1}$ , but its assignment is uncertain.

### K. Bands in the range $1200\text{--}1250 \text{ cm}^{-1}$

In this region, in the absence of other interactions, we expect six bands arising from combinations of  $D_{29}$  and  $D_{11}$ , both with each of the members of the  $(29^2/9^1/11^1)$  Fermi resonance; an expanded version of this region of the REMPI

spectrum is shown at the top of Fig. 10. We recorded ZEKE spectra via each of these bands, with the ZEKE spectra displayed in Fig. 10.

The weak band at  $0^0 + 1208 \text{ cm}^{-1}$  was not seen by KK.<sup>4</sup> It yields a weak ZEKE spectrum with a band at  $1287 \text{ cm}^{-1}$ , which provides a clear assignment to  $29^3$ —see Fig. 10(a). This assigns the intermediate level to the  $29^1 + [29^2 \dots 9^1 \dots 11^2]$  Fermi resonance component. The  $11^1 29^3$  ZEKE band is present but weak and overlapped with accidental resonance bands.

The band at  $0^0 + 1217 \text{ cm}^{-1}$  was also not seen by KK.<sup>4</sup> The ZEKE spectrum recorded via this feature is shown in Fig. 10(b), ZEKE bands at  $856 \text{ cm}^{-1}$  and  $1295 \text{ cm}^{-1}$  may be seen, which are consistent with assignments to  $29^2$  and  $11^1 29^2$ , and hence the intermediate level contains  $11^1 29^2$ . It can be seen that the  $\Delta\nu = -1$  band is the more intense, and weak bands due to  $9^1$  and  $11^2$  are also seen. The activity is consistent with the intermediate level being the  $11^1 + (29^2 \dots 9^1 \dots 11^2)$  Fermi resonance component.

The ZEKE spectrum recorded at  $0^0 + 1224 \text{ cm}^{-1}$ , and shown in Fig. 10(c), is straightforwardly assigned as arising from a  $9^1 29^1$  contribution, with the expected dominance of  $11^1 29^1$ , and  $9^1 29^1$  being the weaker  $\Delta\nu = 0$  band—see Sec. III F and Fig. 4(b); the  $29^3$  band is also present, again in line with expectations. We might expect to see contributions from  $11^2 29^1$ , but these are not obvious in this spectrum (the  $\Delta\nu = 0$  band is expected at  $1310 \text{ cm}^{-1}$ ). The assignment of this

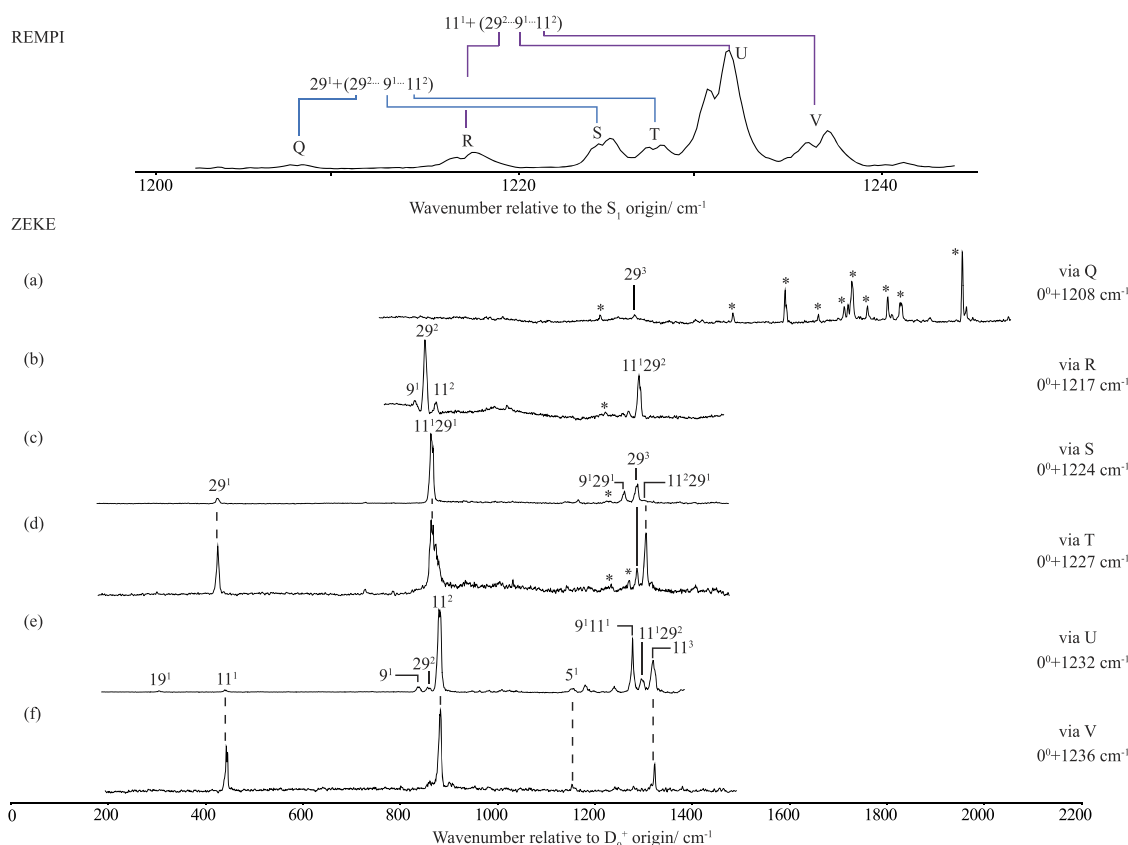


FIG. 10. An expanded view of the  $1202\text{--}1245 \text{ cm}^{-1}$  region of the REMPI spectrum shown in Fig. 1 is presented at the top showing the bands that are used as intermediates in recording the ZEKE spectra presented. See text for discussion of the assignments. Asterisks and obeli ( $\dagger$ ) indicate accidental resonances and are discussed in Sec. III B.

band to the Fermi resonance component  $29^1 + (9^1 \dots 11^2 \dots 29^2)$  then follows. This assignment is consistent with that suggested by KK.<sup>4</sup>

The ZEKE spectrum shown in Fig. 10(d) was recorded at  $0^0 + 1227 \text{ cm}^{-1}$ , and the  $S_1$  level may be straightforwardly assigned as the Fermi resonance component  $29^1 + (11^2 \dots 9^1 \dots 29^2)$ , with the expected dominance of the  $11^n 29^1$  progression.

The ZEKE spectrum recorded at  $0^0 + 1232 \text{ cm}^{-1}$ , and presented in Fig. 10(e), has a clear assignment of  $11^1 + (9^1 \dots 11^2 \dots 29^2)$ , with all of the expected bands (noting again the stronger  $11^2$  and weaker  $9^1 11^1$  bands).

Finally, the ZEKE spectrum recorded via at  $0^0 + 1236 \text{ cm}^{-1}$  is given in Fig. 10(f) and yields an assignment of the  $S_1$  level to  $11^1 + (11^2 \dots 9^1 \dots 29^2)$ .

KK<sup>4</sup> only assigned one of the previous two bands to  $9^1 11^1$ , which was likely our  $1232 \text{ cm}^{-1}$  band as it is the more intense.

Thus, these six REMPI bands seem to be straightforwardly assignable as the expected six combinations. These fall into two distinct groups with the  $29^1$  combinations being of  $b_{3g}$  symmetry, while the  $11^1$  combinations are of  $a_g$  symmetry. It is thus unsurprising, given the absence of any other nearby bands, that the spacings between each set of combinations are essentially the same and concur with those of the parent  $29^2/9^1/11^2$  Fermi resonance triplet.

KK<sup>4</sup> suggested that the  $1236 \text{ cm}^{-1}$  feature may contain contributions from  $16^2$  and  $14^2 18^2$ ; however, both of these would lie outside of the region we scanned and that the former transition is thought to be associated with the REMPI band at  $1252 \text{ cm}^{-1}$  (see Sec. III L and Table I). Thus, these possible additional contributions are still uncertain but seem unlikely.

## L. Bands in the range 1250–1340 $\text{cm}^{-1}$

An expanded version of this region of the REMPI spectrum is shown at the top of Fig. 11. The ZEKE spectrum recorded via  $0^0 + 1252 \text{ cm}^{-1}$ , Fig. 11(a), shows a strong  $\Delta v = 0$  band at  $1689 \text{ cm}^{-1}$ , whose assignment was initially unclear. The appearance of a ZEKE band at  $1378 \text{ cm}^{-1}$ , which can be assigned as  $5^1$ , suggests that the  $1689 \text{ cm}^{-1}$  band comes from a totally symmetric vibration. There are not many possible assignments that are consistent with a  $\Delta v = 0$  shift between the  $S_1$  and  $D_0^+$  states of  $\sim 440 \text{ cm}^{-1}$  except for  $16^2$ ; this would yield a cation value of  $845 \text{ cm}^{-1}$  and an  $S_1$  value of  $626 \text{ cm}^{-1}$ . While the latter is close to the  $619 \text{ cm}^{-1}$  assignment from KK,<sup>4</sup> this came from the assignment of a  $16^1 18^1$  band via the  $1059 \text{ cm}^{-1}$  feature, but we did not see the corresponding ZEKE band (see Sec. III H), casting doubt on that assignment. We favour an assignment of  $16^2$  for the  $1252 \text{ cm}^{-1}$  REMPI band.

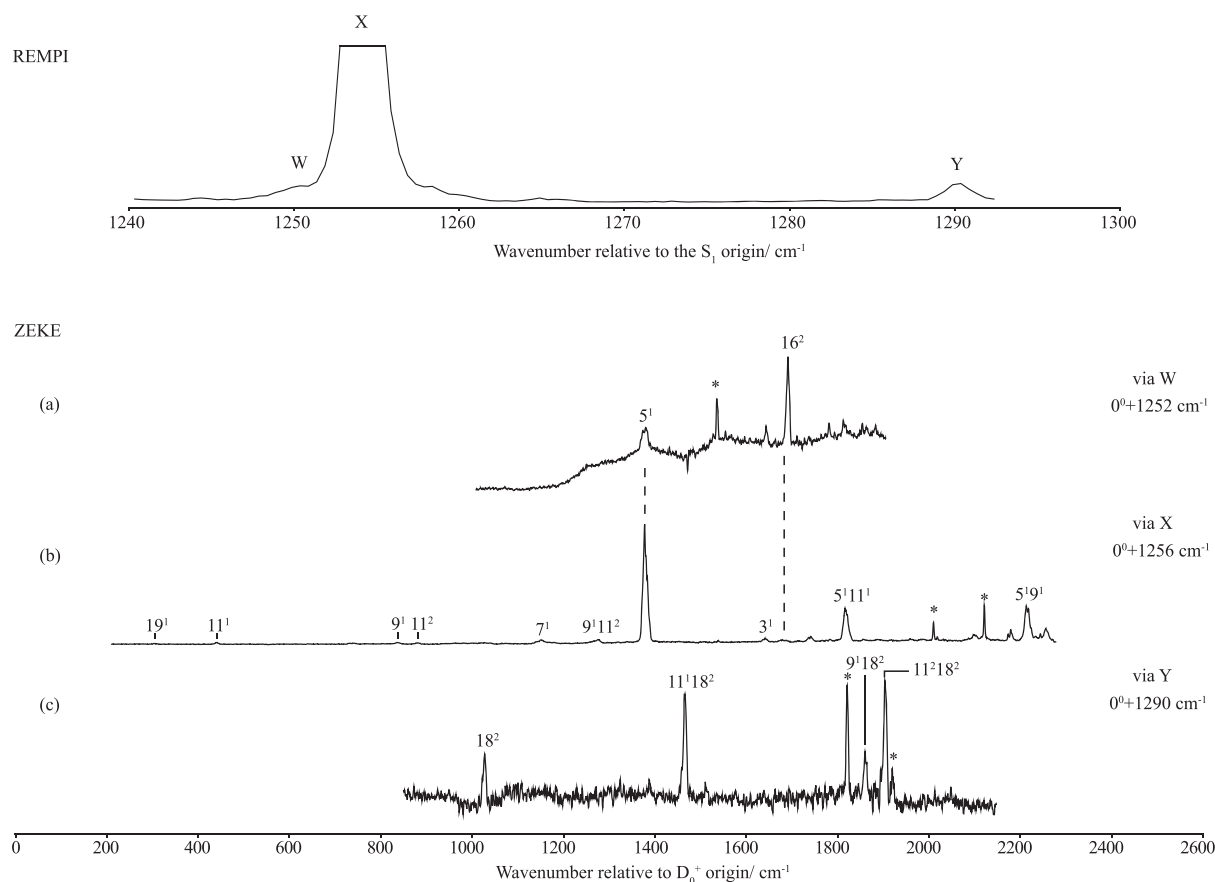


FIG. 11. An expanded view of the  $1240\text{--}1292 \text{ cm}^{-1}$  region of the REMPI spectrum shown in Fig. 1 is presented at the top showing the bands that are used as intermediates in recording the ZEKE spectra presented; note that the  $5^1$  band (marked as X) is off scale—see Fig. 1. See text for discussion of the assignments. Asterisks and obeli (†) indicate accidental resonances and are discussed in Sec. III B.



The ZEKE spectrum obtained when exciting via  $0^0 + 1256\text{ cm}^{-1}$ , Fig. 11(b), yields a strong  $\Delta\nu = 0$  band at  $1377\text{ cm}^{-1}$ , allowing an assignment to  $5^1$ , which concurs with KK.<sup>4</sup> Other bands are straightforwardly assigned to totally symmetric vibrations, with the small band at  $1689\text{ cm}^{-1}$  suggesting a weak  $5^1 \dots 16^2$  Fermi resonance. Interestingly, we see the  $9^1$  vibronically induced band, but not  $14^1$ . Although time-resolved photoelectron spectra were recorded via the coherent excitation of the  $1252$  and  $1256\text{ cm}^{-1}$  bands in the present work, no time dependence was observed, suggesting that any coupling with  $16^2$  is weak.

The ZEKE spectrum obtained when exciting via  $0^0 + 1290\text{ cm}^{-1}$ , Fig. 11(c), yields two strong bands that can be assigned as  $11^1 18^2$  and  $11^2 18^2$ , with the  $S_1$  excitation position allowing an assignment to the intermediate as  $11^1 18^2$  in agreement with KK.<sup>4</sup> We also see the totally symmetric bands  $18^2$  and  $9^1 18^2$ .

## IV. FURTHER DISCUSSION

### A. Fermi resonances

The Fermi resonance between the  $9^1$  and  $11^2$  levels has been discussed by CP<sup>3</sup> and KK.<sup>4</sup> As may be seen from the expanded view of this region of the REMPI spectrum at the top of Fig. 4, bands B and C are very close together, with a third, band A, to lower wavenumber. CP<sup>3</sup> scanned across the region corresponding to bands B and C recording DF spectra. They found that the  $11_2$  activity was dominant when exciting to higher wavenumber, while  $9_1$  was more active to lower wavenumber (which is in-line with our ZEKE spectra). This, and the presence of bands associated with both transitions in all spectra, led them to the conclusion that bands B and C (in the REMPI spectrum of Fig. 4) comprised a Fermi resonance. This conclusion was also supported by KK,<sup>4</sup> and both papers also provided some explanation of the surprisingly intense  $11_1$  band in the DF spectra.

In the present work—see Sec. III F—we concur with the above, but we also conclude that the  $S_1$   $29^2$  band is part of the Fermi resonance, consistent with the Fermi resonance between  $9^1$  and  $29^2$  seen in pFT,<sup>27,39</sup> where these two levels are very close together. The ZEKE spectra suggest that both the  $9^1 \dots 29^2$  and  $9^1 \dots 11^2$  interactions are significant, while the  $29^2 \dots 11^2$  interaction is weak. The latter may be viewed as a Darling-Dennison interaction, but interestingly the interaction is not direct but appears only to occur by virtue of the pairwise interactions with  $9^1$ .

As noted above, we also studied this Fermi resonance using time-resolved photoelectron spectroscopy using picosecond laser pulses. This work confirmed that the main interaction was between the  $9^1$  and  $11^2$  levels but implied a weak interaction with the  $11^1 29^1$  level, probably by Herzberg-Teller coupling. Since we do not see any evidence of such coupling between  $11^1$  and  $29^1$ —see Sec. III D and Fig. 2—then the interaction must be directly with the  $9^1$  zero-order bright state.

We now comment on a time-resolved study by Long *et al.*<sup>41</sup> In that work, a 45 fs UV pulse ( $266.7\text{ nm}$ ) was used to excite the  $S_1 \leftarrow S_0$  transition and then after a delay of tens of picoseconds, multiple photons from a second pulse

( $\sim 800\text{ nm}$ ) ionized the molecule; photoelectron spectra were then recorded and their variation with time delay was used as a probe of the dynamical processes occurring in the  $S_1$  state. The pulse width corresponds to  $\sim 490\text{ cm}^{-1}$  meaning that vibrational selectivity is limited. In that work,<sup>41</sup> it was concluded that it was likely that the  $11^1$  and  $9^1$  modes were excited, and since they were referring to the work by CP<sup>3</sup> and KK,<sup>4</sup> the  $9^1$  transition was noted as being the  $9^1 \dots 11^2$  Fermi resonance (while we conclude here that there is involvement from  $29^2$  also). Owing to this poor energy resolution, it was difficult to interpret the photoelectron spectrum presented in Ref. 41, which was thought to consist of contributions from both exciting via  $11^1$  and the  $9^1 \dots 11^2$  Fermi resonance (although it seems that the former transition would only just be caught by the wings of the laser pulse); additionally, the resolution of the photoelectron spectrum seems to be  $>700\text{ cm}^{-1}$ . Furthermore, the two photoelectron bands that resulted from ionization from the Fermi resonance levels appear to correspond to levels of the ion that lie far above the AIE. These aspects led the authors to conclude that the assignment of the intermediate level was far from clear, but they did see oscillations of photoelectron band intensities that had a period consistent with the separation of the  $9^1$  and  $11^2$  levels.

The three bands in the  $930\text{--}960\text{ cm}^{-1}$  range, see Sec. III G, also arise from a three-way Fermi resonance between  $15^1 19^1$ ,  $13^2$ , and  $20^2 30^2$ . All three  $\Delta\nu = 0$  features appear in each of the ZEKE spectra exciting via each of these bands, and the relative intensities suggest that all three eigenstates are quite mixed. As we indicated above, there is an unidentified ZEKE band at  $1286\text{ cm}^{-1}$  that appears to arise from an  $S_1$  level that does not form part of the interactions. In addition, the  $954\text{ cm}^{-1}$  feature contains a clear overlapped transition with  $11^1 19^2$ , together with the weak  $28^1 29^1$ . On the basis of quantum number changes,  $\Delta N$ , in particular that small differences in vibrational quantum number between coupled levels are favoured,<sup>42</sup> it may have been expected that the  $11^1 19^2$  and  $15^1 19^1$  bands would interact strongly, but this does not seem to be the case. By the same argument, it is surprising that there is apparently strong mixing between the  $15^1 19^1$ ,  $13^2$ , and  $20^2 30^2$  levels, where  $\Delta N = 4$  or  $6$ .

The  $1059\text{ cm}^{-1}$  feature, see Sec. III H, was found to comprise a  $17^2 \dots 14^1 17^1 30^1$  Fermi resonance, as well as an overlapping  $9^1 20^2$  contribution. Interestingly, the  $9^1 20^2$  band seems cleanest on the low-wavenumber side of the band, but there is not the switch in intensity to the  $11^2 20^2$  band (at  $1140\text{ cm}^{-1}$ ), which the underlying  $29^2/9^1/11^2$  Fermi resonance would suggest, although there is significant broadening. Finally, we see no clear evidence for the  $16^1 18^1$  band in the ZEKE spectrum, which was suggested as being present by KK,<sup>4</sup> and although we cannot conclusively rule out the possibility that its contribution is narrow in wavenumber and that we missed this, it seems unlikely.

The bands that occur in the  $1160\text{--}1195\text{ cm}^{-1}$  region—see the top of Fig. 9—are very interesting in that they are made up of two overlapping Fermi resonances of the same symmetry (see Sec. III J), yet they appear to be almost completely distinct. The first of these comprises four levels that are made up of the  $14^2$  in combination with each of the three  $29^2/9^1/11^2$  Fermi resonance levels, and also  $14^1 18^1 28^1$ . These

are then overlapped with a two-component Fermi resonance,  $11^1 12^1 14^1 \dots 12^2$ . The ZEKE spectra clearly indicate the contributing eigenstates, allowing this complicated picture to be unravelled.

We have also unpicked the assignments of the bands in the range  $1205\text{--}1240\text{ cm}^{-1}$ —see the top of Fig. 10 and Sec. III K—which are found to comprise six bands, made up of two distinct complex Fermi resonances:  $29^1$  in combination with each of the  $29^2/9^1/11^2$  Fermi resonance components, and corresponding component bands between  $11^1$  and  $29^2/9^1/11^2$ . These two sets of three levels have  $b_{3g}$  and  $a_g$  symmetry, respectively, and hence are not expected to interact directly; this is borne out by the ZEKE spectra.

As well as the  $9^1 \dots 11^2$  Fermi resonance discussed in the KK<sup>4</sup> paper, aspects of the other abovementioned Fermi resonances are commented on in the supplementary information of that work, as noted in the above text, although not all of the bands discussed in the present work were seen.

## B. Vibronic coupling

### 1. $S_1 \leftarrow S_0$ transition

The  $S_1 \ ^1B_{2u} \leftarrow S_0 \ ^1A_{1g}$  transition in benzene is a classic case of Herzberg-Teller coupling, where the transition is electric-dipole forbidden, but becomes allowed via vibronic interactions that may be viewed as intensity stealing of the  $S_1$  state from a higher electric-dipole allowed  $^1E_{1u}$  state. The vibronic interaction induces activity in vibrations of  $e_{2g}$  symmetry in the  $S_1$  state. Benzene has the outermost  $\pi$  electronic configuration  $\dots a_{2u}^2 e_{1g}^2 e_{2u}^0 b_{2g}^0$ . The degeneracies of the  $e$  orbitals are lost in  $D_{2h}$ , and this  $\pi$  electronic configuration becomes  $\dots b_{3u}^2 b_{1g}^2 b_{2g}^2 a_u^0 b_{3u}^0 b_{2g}^0$  for  $p\text{DFB}$ , although other low-lying unoccupied orbitals may be present. Although the  $S_1 \leftarrow S_0$  transition, corresponding to an  $a_u \leftarrow b_{2g}$  excitation, becomes allowed under  $D_{2h}$  point group symmetry, vibronic coupling can still occur and this leads to activity in  $b_{3g}$  modes; in particular, the  $D_{29}$  vibration appears to be the most active and the  $29^1$  band is seen clearly in the REMPI spectrum in Fig. 1, with the  $28^1$  transition also being seen but weaker. Although transitions involving  $a_g$  vibrations are Franck-Condon allowed, in principle the intensities of these can be affected by vibronic coupling.<sup>36</sup> The observation of non-Franck-Condon active modes opens up the ability to obtain information on the corresponding vibrations of the cation.

KK<sup>4</sup> commented on the possible role of other coupling mechanisms in the  $S_1$  state, partly justified by the observation of combination bands of overall  $a_g$  symmetry, but involving non-totally symmetric modes (such as  $12^1 14^1$ ); the large change in wavenumber of some vibrations between the  $S_0$  and  $S_1$  states; and the change in vibrational activity between one-photon and two-photon electronic spectra. In principle, combination bands can occur as the result of anharmonic (Fermi resonance) coupling and the large changes in wavenumber appear to be the result of electronic structure changes [e.g., the calculated wavenumber of the  $D_{14}$  mode of (mono)fluorobenzene is much higher in the  $S_1$  state than the  $S_0$  state in the absence of any vibronic coupling<sup>43</sup> and is in good agreement with the experimental value]. The difference in one-

and two-photon electronic spectra has also been discussed by Blease *et al.*<sup>36</sup> and also attributed to vibronic coupling.

### 2. $D_0^+ \leftarrow S_1$ transition

In the low-wavenumber region of the ZEKE spectrum obtained when exciting via the  $S_1$  origin, as well as a number of  $S_1$  totally symmetric modes, we observe three main Franck-Condon-forbidden bands,  $D_{20}$ ,  $D_{19}$ , and  $D_{14}$ , which have respective symmetries  $b_{3u}$ ,  $b_{2g}$ , and  $a_u$ .

If we consider the ionization involving the vibronic levels of the  $S_1$  and  $D_0^+$  states, ignoring the departing electron, then the transition moment will be given by

$$\langle \psi'_{ev} | \mu | \psi_{ev}^+ \rangle. \quad (2)$$

Taking into account the electronic symmetries of the  $S_1$  and  $D_0^+$  states, as well as the symmetries of the three components of  $\mu$ , then the symmetry condition for a vibronically allowed transition may be derived to be

$$\Gamma(\psi'_v) \times \Gamma(\psi_v^+) \supseteq b_{1g}, b_{2g}, b_{3g}, \quad (3)$$

but this would only be consistent with ionization to the  $19^1$  level becoming allowed, when exciting from an  $S_1$  totally symmetric vibrational level, such as the zero-point level. Even then, the vibronic transition would have to steal intensity from an excited ( $B_{2g} \times b_{2g} =$ )  $A_g$  cationic state via a Herzberg-Teller mechanism, and no such state exists low enough in energy<sup>15</sup> for this to be viable.

We now consider the case where we view the ZEKE process as an excitation to a high-lying Rydberg state. First of all, we note that the symmetries of a Rydberg electron in  $D_{2h}$  symmetry are<sup>9</sup>

$$s : a_g(s\sigma),$$

$$p : b_{1u}(p\sigma); b_{2u} + b_{3u}(p\pi),$$

$$d : a_g(d\sigma); a_g + b_{1g}(d\pi); b_{2g} + b_{3g}(d\delta),$$

$$f : b_{1u}(f\sigma); b_{2u} + b_{3u}(f\pi); a_u + b_{1u}(f\delta); b_{2u} + b_{3u}(f\phi).$$

As such, and as stated in Ref. 9, these cover all of the  $D_{2h}$  symmetry classes, and so in principle it is possible to combine the symmetry of the cation wavefunction with that of an appropriate Rydberg electron to yield a Rydberg state of the correct symmetry to undergo Herzberg-Teller intensity stealing from any low-lying excited state. The lowest-lying cationic state is of  $B_{1g}$  symmetry at  $\sim 1$  eV, with other states at lying  $> 2.7$  eV.<sup>15</sup> So if we assume it is Herzberg-Teller coupling between Rydberg states that have  $^2B_{2g}$  (i.e.,  $D_0^+$ ) and  $^2B_{1g}$  cationic cores that causes the observation of the three Franck-Condon-forbidden vibrations,  $D_{20}$ ,  $D_{19}$ , and  $D_{14}$ , then we can deduce an appropriate choice of the Rydberg electron in which each of these would lead to an allowed transition, and then can consider whether this is a viable Herzberg-Teller interaction involving the  $B_{1g}$  cation state—or rather the Rydberg states thereof.

The allowed symmetries of the Rydberg electron,  $\Gamma(\psi_{\text{Ryd}})$ , that may be excited from the  $S_1$  state can be deduced from

$$\begin{aligned} \Gamma(\psi_{\text{Ryd}}) &= \Gamma(\psi_e, S_1) \times \Gamma(\psi_{\text{vib}}, S_1) \times \Gamma(\mu) \\ &\quad \times \Gamma(\psi_e, D_0^+) \times \Gamma(\psi_{\text{vib}}, D_0^+), \end{aligned} \quad (4)$$

which simplifies to

$$\Gamma(\Psi_{\text{Ryd}}) = (b_{1g}, b_{2g}, b_{3g}) \times \Gamma(\Psi_{\text{vib}}, D_0^+). \quad (5)$$

Hence, for activity in the  $D_{19}$  vibration when exciting from the  $S_1$  vibrationless level, we would require  $\Gamma(\Psi_{\text{Ryd}}) = (b_{3g}, a_g, b_{1g})$ , with the corresponding symmetries for  $D_{20}$  and  $D_{14}$  being  $(b_{2u}, b_{1u}, a_u)$  and  $(b_{1u}, b_{2u}, b_{3u})$ .

It seems reasonable to assume that if the electronic symmetry of the Rydberg state is pertinent and is obtained from the combination of the cation core and the Rydberg electron, then the Rydberg electron and the electrons of the cationic core should interact. This suggests that the coupling will be strongest if the Rydberg electron is s or p, in both Rydberg states, which are the most penetrating. (Although subsequent  $l$  and  $m_l$  mixing may occur,<sup>44</sup> this will be subsequent to the transition to the Rydberg state.) So, for the  $D_{19}$  mode, this would require the Rydberg electron to be s, and so the Rydberg vibronic symmetry to be  $B_{2g} \times b_{2g} \times a_g = A_g$ . As already noted, the lowest cationic excited state is of  $B_{1g}$  symmetry,<sup>15</sup> and so when combined with Rydberg symmetries for s and p electrons, this yields Rydberg state symmetries of  $B_{1g}, A_u, B_{3u}$ , and  $B_{2u}$ , none of which are of the correct symmetry to interact with the  $D_0^+ 19^1$  vibronic level. As such, the Herzberg-Teller mechanism does not appear to be viable for  $19^1$ . In a similar way,  $D_{20}$  would require a p electron, and to have Rydberg vibronic symmetries of  $B_{2g} \times b_{3u} \times b_{1u} = A_g$  or  $B_{2g} \times b_{3u} \times b_{2u} = B_{3g}$ , with neither of these being able to couple to the Rydberg states of lowest-lying excited cation state. Finally, in a similar way,  $D_{14}$  would require a p electron and have Rydberg vibronic symmetries of  $B_{2g} \times a_u \times b_{1u} = B_{3g}$ ,  $B_{2g} \times a_u \times b_{2u} = A_g$ , or  $B_{2g} \times a_u \times b_{3u} = B_{1g}$ , with only the latter one being viable. Hence, although vibronic coupling is a possible explanation for the activity of  $14^1$ , it is not viable for  $19^1$  or  $20^1$ .

At this point, we also note that the same Franck-Condon-forbidden vibrations appear in the low wavenumber region of the one-colour MATI spectrum of Kwon *et al.*,<sup>11</sup> with what appear to be similar intensities. Since the ionization there occurs from the  $S_0$  state, which has  $A_g$  symmetry, then this modifies the symmetry arguments. For example, excitation to p Rydberg states is possible for  $19^1$ , giving the Rydberg vibronic symmetries as  $B_{2g} \times b_{2g} \times b_{1u} = B_{1u}$ ,  $B_{2g} \times b_{2g} \times b_{2u} = B_{2u}$  or  $B_{2g} \times b_{2g} \times b_{3u} = B_{3u}$ , with two of these allowing Herzberg-Teller interaction with the Rydberg states arising from the  $B_{1g}$  excited cationic core and a p Rydberg electron. However,  $20^1$  would require an s electron, and so a Rydberg vibronic symmetry of  $B_{2g} \times b_{3u} \times a_g = B_{1u}$ , which cannot interact with the lowest excited Rydberg states. In a similar way,  $14^1$  requires an s electron, and a Rydberg vibronic symmetry of  $B_{2g} \times a_u \times a_g = B_{2u}$ —which can interact with the excited Rydberg states. Hence, although vibronic coupling is now a possible explanation for the activity of  $14^1$  and  $19^1$ , it does not appear to be viable for  $20^1$ .

Herzberg-Teller coupling is an intensity stealing mechanism resulting from vibronic interactions between electronic states and is termed interchannel coupling. Poliakoff, Lucchese, and co-workers have recently been developing the idea of intrachannel coupling,<sup>45</sup> initially as an explanation for the activity of Franck-Condon-forbidden  $\pi$  bending vibrations

in the photoelectron spectra of  $\text{CO}_2$ .<sup>46</sup> This work has now been expanded to other molecules, and some attention has been given to polyatomic molecules<sup>47</sup> and applied by others to chiral molecules.<sup>48</sup> The theory does not depend on the Herzberg-Teller intensity stealing mechanism but does depend on the non-separability of the electronic and nuclear motion, in requiring the transition moment for ionization to be dependent on the vibrational motion. The mechanism effectively involves the departing electron interacting with the potential of the core, which has a vibrational dependence; as such, the symmetry of the departing electron is brought into the argument but does not require any intensity stealing to be invoked.<sup>45,47</sup> In the present work, we have extended these arguments to include the formation of high-lying Rydberg states that are populated in ZEKE experiments. Of note is that the three non-Franck-Condon-active modes,  $D_{20}$ ,  $D_{19}$ , and  $D_{14}$ , have the lowest wavenumber of all of the modes of  $p\text{DFB}$  and so may reasonably be expected to have the largest nuclear displacement during their vibrations.

In summary, we hypothesise that the intrachannel coupling mechanism applies to the ZEKE Rydberg states prior to any  $l$  and  $m_l$  mixing and field ionization and that s and p Rydberg electrons are expected to couple more strongly with the  $D_0^+$  core. We then assume the Rydberg states must satisfy both the symmetry requirements for the excitation step from the intermediate level, and those for intrachannel vibronic coupling. The important point is that the position and symmetry of higher cationic states are now irrelevant. This would explain the similar non-Franck-Condon activity for both the two-colour ZEKE and the one-colour MATI spectra referred to above. Also, in the conventional photoelectron spectrum in Fig. 5(a), there do appear to be contributions from non-Franck-Condon vibrations between the  $0^0$  and  $11^1$  bands, although it is not possible to say whether all three vibrations are active.

From Table I, it can be seen that  $D_{30}$  has a wavenumber similar to that of  $D_{14}$  in the cation, and so it may be wondered why this is not active. We note that  $D_{30}$  is an in-plane vibration (see Table I and Ref. 25), and the ionization is occurring from a  $\pi$  or  $\pi^*$  orbital in the case of the  $S_0$  and  $S_1$  states, respectively. As such, it seems more likely that out-of-plane vibrations will interact with the outgoing electron, and so become active.

### 3. Vibrational wavenumbers

The vibrational wavenumbers of the  $S_0$  state have been discussed in detail in Ref. 25. We also made some comments on the vibrational wavenumbers of the  $S_1$  state of  $p\text{DFB}$  in Ref. 27 in relation to those of  $p\text{FT}$ . To that discussion, we add here that we believe we have strong evidence for the  $7^1$  transition at  $1114 \text{ cm}^{-1}$  and so can confirm the provisional assignment given by KK.<sup>4</sup> In addition, we confirm many other  $S_1$  wavenumbers. For all  $S_1$  vibrational wavenumbers that have been determined or confirmed in our work, the agreement between the calculated and experimental values is good, except for  $D_{14}$ , which we have pointed out in earlier work<sup>26,27,35</sup> is poorly described by DFT methods. The agreement is fair for two other experimentally determined values (see Table I),  $D_{10}$  and  $D_{27}$ , which were not confirmed in the present work. On the other hand,

the agreement for one  $a_g$ , two  $b_{3g}$ , and one  $b_{2u}$  modes is exceptionally poor:  $D_4$ ,  $D_{23}$ ,  $D_{25}$ , and  $D_{26}$ . The first three of these come from the two-photon study of RS,<sup>2</sup> while the last was put forward by KK.<sup>4</sup> We have discussed the 1286  $\text{cm}^{-1}$  ZEKE band observed via the 933  $\text{cm}^{-1}$  intermediate  $S_1$  level in Sec. III G. Although we have an assignment for the 933  $\text{cm}^{-1}$  feature, we presently assume that there is an unidentified overlapping feature here that gives rise to the (also unidentified) 1286  $\text{cm}^{-1}$  ZEKE band (although either  $9^1 11^1$  or  $29^3$  are possible assignments for this band, neither is expected with this intensity via this feature). Currently, therefore, the assignment of the  $D_4$ ,  $D_{23}$ ,  $D_{25}$ , and  $D_{26}$  vibrations must remain tentative.

We now move onto the cation. As with the  $S_0$  state, we expect the calculated wavenumbers to be in good agreement with the experimentally derived values, and this is true for all of the values derived from the ZEKE spectra, many of which are consistent with those from the other ZEKE or MATI studies. In the one-photon MATI spectrum of Ref. 11, values for most of the cation vibrations were given, but assignments could only be based upon the calculated wavenumbers, combined with expectations that totally symmetric vibrations were the most active. That said, a number of the assignments were uncertain and we feel that the assignments of a number of the non-totally symmetric vibrations are incorrect. For example, the values assigned in Ref. 11 to vibrations  $D_{22}$ – $D_{27}$  (see Table I) could be assigned, respectively, to the totally symmetric modes  $5^1 9^2$ ,  $17^2$ ,  $9^1 11^1 20^2$ ,  $16^1 18^1$  or  $19^2 30^2$ ,  $9^1 11^1$ , and  $20^2 29^2$ . Additionally, values of 743/731  $\text{cm}^{-1}$  that were suggested as being assignable to  $D_{10}$  or  $D_{17}$  could be assigned to  $30^2$  and  $14^2$ , while the 1015  $\text{cm}^{-1}$  value given for  $D_{12}$  or  $D_{15}$  is possibly  $28^1 29^1$ . Also, given the comments in Sec. IV B and the results of the present work, the band observed with a wavenumber of 368  $\text{cm}^{-1}$  that was suggested in Ref. 11 as being either  $D_{14}$  or  $D_{30}$  is likely the former. These reassignments are much more in line with the expected symmetries of active vibrations, even taking into account vibronic coupling.

Finally, we also pointed out in Sec. III J that the previous value of 726  $\text{cm}^{-1}$  assigned to  $D_{13}$  in the cation<sup>9</sup> was incorrect, and similarly that the value of 859  $\text{cm}^{-1}$  ascribed to  $D_{16}$  in Ref. 11 and taken from Ref. 10 is an incorrect assignment, with the authors of Ref. 10 suggesting three possible assignments; one of these was  $29^2$ , which is the assignment we are confident of from the present ZEKE results.

## V. CONCLUDING REMARKS

In this work, we have presented ZEKE spectra recorded via all significant  $S_1$  levels that are active in the 0–1300  $\text{cm}^{-1}$  region of the one-photon  $S_1 \leftarrow S_0$  transition. In so doing, we have been able to confirm the assignments of almost all bands discussed by Knight and Kable<sup>4</sup> but have clarified some of these while uncovering a number of complex Fermi resonances, some of which are associated with bands not explicitly mentioned in Ref. 4. This has also allowed the confident confirmation or establishment of the wavenumbers of seventeen vibrations in the  $D_0^+$  state. Many of these vibrations have been identified as  $\Delta v = 0$  bands in ZEKE spectra

and are seen across a number of spectra, giving weight to their assignments; that the results are also in good agreement with the calculated values which gives additional credence to these.

Statistical (or dissipative) IVR is expected to occur at  $>2000 \text{ cm}^{-1}$  in  $p\text{DFB}$ .<sup>4</sup> In the present work, we have seen examples of the sporadic build-up of vibrational coupling via the identification of a number of complex Fermi resonances at  $<1300 \text{ cm}^{-1}$ . This sporadic nature of the build-up of the density of states was highlighted in recent work.<sup>39</sup> It is also interesting that, although there was the expected non-interaction between overlapping Fermi resonance features of different symmetry, there were cases of components of the same symmetry overlapping but not interacting (see Sec. III J), suggesting the coupling of zero-order states also depends on the relative motions of the vibrations, as well as their symmetry.

We have also considered the appearance of non-Franck-Condon-allowed vibrations in the low-wavenumber region of the ZEKE spectrum recorded via the  $S_1$  origin. We extended the arguments of Ref. 45 to include high-lying Rydberg states and suggest that  $ns$  and  $np$  Rydberg states are more likely to be involved in intrachannel coupling. We have also suggested that for ionization from  $\pi$  or  $\pi^*$  orbitals in substituted benzenes, it is more likely that out-of-plane vibrations will lead to such interactions.

## ACKNOWLEDGMENTS

We are grateful to the EPSRC for funding (Grant Nos. EP/L021366/1 and EP/E046150). The EPSRC and the University of Nottingham are thanked for studentships to W.D.T., D.J.K., and J.M. The High Performance Computer resource at the University of Nottingham was employed for the quantum chemistry calculations.

<sup>1</sup>C. D. Cooper, *J. Chem. Phys.* **22**, 503 (1954).

<sup>2</sup>M. J. Robey and E. W. Schlag, *Chem. Phys.* **30**, 9 (1978).

<sup>3</sup>R. A. Coveleskie and C. S. Parmenter, *J. Mol. Spectrosc.* **86**, 86 (1981).

<sup>4</sup>A. E. W. Knight and S. H. Kable, *J. Chem. Phys.* **89**, 7139 (1988). Note that this work includes a significant number of further spectra and comments as part of the supplementary material.

<sup>5</sup>Q. Ju, C. S. Parmenter, T. A. Stone, and Z.-Q. Zhao, *Isr. J. Chem.* **37**, 379 (1997).

<sup>6</sup>E. Sekreta, K. S. Viswanathan, and J. P. Reilly, *J. Chem. Phys.* **90**, 5349 (1989).

<sup>7</sup>S. M. Bellm and K. L. Reid, *Chem. Phys. Lett.* **395**, 253 (2004).

<sup>8</sup>D. Rieger, G. Reiser, K. Müller-Dethlefs, and E. W. Schlag, *J. Phys. Chem.* **96**, 12 (1992).

<sup>9</sup>G. Reiser, D. Rieger, T. G. Wright, K. Müller-Dethlefs, and E. W. Schlag, *J. Phys. Chem.* **97**, 4335 (1993).

<sup>10</sup>G. Lembach and B. Brutschy, *J. Phys. Chem. A* **102**, 6068 (1998).

<sup>11</sup>C. H. Kwon, H. L. Kim, and M. S. Kim, *J. Chem. Phys.* **118**, 6327 (2003).

<sup>12</sup>V. E. Bondybey, T. A. Miller, and J. H. English, *J. Chem. Phys.* **72**, 2193 (1980).

<sup>13</sup>Y. Tsuchiya, M. Fujii, and M. Ito, *J. Chem. Phys.* **90**, 6965 (1989).

<sup>14</sup>Y. Tsuchiya, M. Fujii, and M. Ito, *Chem. Phys. Lett.* **168**, 173 (1990).

<sup>15</sup>S.-Y. Yu and M.-B. Huang, *J. Mol. Struct.: THEOCHEM* **822**, 48 (2007).

<sup>16</sup>D. Boyall and K. L. Reid, *Chem. Soc. Rev.* **26**, 223 (1997).

<sup>17</sup>K. L. Reid, *Int. Rev. Phys. Chem.* **27**, 607 (2008).

<sup>18</sup>J. A. Davies, A. M. Green, A. M. Gardner, C. D. Withers, T. G. Wright, and K. L. Reid, *Phys. Chem. Chem. Phys.* **16**, 430 (2014).

<sup>19</sup>S. D. Gamblin, S. E. Daire, J. Lozeille, and T. G. Wright, *Chem. Phys. Lett.* **325**, 232 (2000).

- <sup>20</sup>V. L. Ayles, C. J. Hammond, D. E. Bergeron, O. J. Richards, and T. G. Wright, *J. Chem. Phys.* **126**, 244304 (2007).
- <sup>21</sup>X. Zhang, J. M. Smith, and J. L. Knee, *J. Chem. Phys.* **97**, 2843 (1992).
- <sup>22</sup>J. A. Davies, A. M. Green, and K. L. Reid, *Phys. Chem. Chem. Phys.* **12**, 9872 (2010).
- <sup>23</sup>J. Midgley, J. A. Davies, and K. L. Reid, *J. Phys. Chem. Lett.* **5**, 2484 (2014).
- <sup>24</sup>J. Midgley, J. A. Davies, and K. L. Reid, *J. Chem. Phys.* **139**, 117101 (2013).
- <sup>25</sup>A. Andrejeva, A. M. Gardner, W. D. Tuttle, and T. G. Wright, *J. Mol. Spectrosc.* **321**, 28 (2016).
- <sup>26</sup>W. D. Tuttle, A. M. Gardner, K. B. O'Regan, W. Malewicz, and T. G. Wright, *J. Chem. Phys.* **146**, 124309 (2017).
- <sup>27</sup>W. D. Tuttle, A. M. Gardner, L. E. Whalley, and T. G. Wright, *J. Chem. Phys.* **146**, 244310 (2017).
- <sup>28</sup>T. Cvitaš and J. M. Hollas, *Mol. Phys.* **18**, 793 (1970).
- <sup>29</sup>W. D. Tuttle, A. M. Gardner, and T. G. Wright, *Chem. Phys. Lett.* **684**, 339 (2017).
- <sup>30</sup>R. S. Mulliken, *J. Chem. Phys.* **23**, 1997 (1955).
- <sup>31</sup>G. Herzberg, *Molecular Spectra and Molecular Structure. II. Infrared and Raman Spectra of Polyatomic Molecules* (Krieger, Malabar, 1991).
- <sup>32</sup>E. B. Wilson, Jr., *Phys. Rev.* **45**, 706 (1934).
- <sup>33</sup>G. Varsányi, *Assignments of the Vibrational Spectra of Seven Hundred Benzene Derivatives* (Wiley, New York, 1974).
- <sup>34</sup>M. Fujii, T. Kakinuma, N. Mikami, and M. Uto, *Chem. Phys. Lett.* **127**, 297 (1986).
- <sup>35</sup>D. J. Kemp, L. E. Whalley, W. D. Tuttle, A. M. Gardner, B. T. Speake, and T. G. Wright, *Phys. Chem. Chem. Phys.* **20**, 12503 (2018).
- <sup>36</sup>T. G. Blease, R. J. Donovan, P. R. R. Langridge-Smith, and T. R. Ridley, *Laser Chem.* **9**, 241 (1988).
- <sup>37</sup>Z.-Q. Zhao and C. S. Parmenter, *Ber. Bunsenges. Phys. Chem.* **99**, 536 (1995).
- <sup>38</sup>J. A. Davies and K. L. Reid, *Phys. Rev. Lett.* **109**, 193004 (2012).
- <sup>39</sup>W. D. Tuttle, A. M. Gardner, L. E. Whalley, D. J. Kemp, and T. G. Wright, *Phys. Chem. Chem. Phys.* (to be published).
- <sup>40</sup>A. M. Gardner, W. D. Tuttle, L. E. Whalley, and T. G. Wright, *Chem. Sci.* **9**, 2270 (2018).
- <sup>41</sup>J. Long, C. Qin, Y. Liu, S. Zhang, and B. Zhang, *Phys. Rev. A* **84**, 063409 (2011).
- <sup>42</sup>N. T. Whetton and W. D. Lawrance, *J. Phys. Chem.* **93**, 5377 (1989).
- <sup>43</sup>I. Pugliesi, N. M. Tonge, and M. C. R. Cockett, *J. Chem. Phys.* **129**, 104303 (2008).
- <sup>44</sup>See, for example, W. A. Chupka, *J. Chem. Phys.* **98**, 4520 (1993).
- <sup>45</sup>G. J. Rathbone, E. D. Poliakoff, J. D. Bozek, and R. R. Lucchese, *Can. J. Chem.* **82**, 1043 (2004).
- <sup>46</sup>J. S. Miller, E. D. Poliakoff, T. F. Miller III, A. P. Natalense, and R. R. Lucchese, *J. Chem. Phys.* **114**, 4496 (2001).
- <sup>47</sup>E. D. Poliakoff and R. R. Lucchese, *Phys. Scr.* **74**, C71 (2006).
- <sup>48</sup>G. A. Garcia, H. Dossmann, L. Nahon, S. Daly, and I. Powis, *ChemPhysChem* **18**, 500 (2017).